# Synthesis, in vitro and in vivo biological evaluation of novel dual compounds targeting both acetylcholinesterase and serotonergic 5-HT4 receptors with potential interest in the treatment of Alzheimer's disease

Christophe Rochais, Cédric Lecoutey, Julien Lalut, Audrey Davis, Emilie Duval, Florence Gaven, Stacy Largillière, Gérald Née, Sophie Corvaisier, Jana Sopkova de Oliveira Santos, et al.

European Journal of Medicinal Chemistry 280 (2024) 116975

Contents lists available at ScienceDirect

European Journal of Medicinal Chemistry

journal homepage: www.elsevier.com/locate/ejmech

Research paper

# Synthesis, *in vitro* and *in vivo* biological evaluation of novel dual compounds targeting both acetylcholinesterase and serotonergic 5-$HT_4$ receptors with potential interest in the treatment of Alzheimer's disease

Christophe Rochais [a,**], Cédric Lecoutey [a], Julien Lalut [a], Audrey Davis [a], Emilie Duval [a], Florence Gaven [c,1], Stacy Largillière [b], Gérald Née [b], Sophie Corvaisier [a], Jana Sopkova de Oliveira Santos [a], Marc Since [a,d], Thomas Freret [b], Romain Legrand [e], Noëlle Callizot [f], Sylvie Claeysen [c], Michel Boulouard [b], Patrick Dallemagne [a,*]

[a] Université de Caen Normandie, Normandie Univ., Centre d'Etudes et de Recherche sur le Médicament de Normandie (CERMN), 14000 Caen, France
[b] Université de Caen Normandie, Normandie Univ., Mobilités: Vieillissement, Pathologie, Santé (COMETE), INSERM UMR-S 1075, 14000, Caen, France
[c] IGF, Univ. Montpellier, CNRS, INSERM, F-34094, Montpellier, France
[d] PRISMM Platform, PLATON Service Unit, Caen, Université de Caen Normandie, France
[e] RONOMA Pharma, 31 Rue Léon Delille, F-76800, Saint Etienne du Rouvray, France
[f] Neuro-Sys, 410 Chemin départemental 60, F-13120, Gardanne, France

ARTICLE INFO

*Keywords:*
Alzheimer's disease
Pleiotropic
Acetylcholinesterase
Serotonin
5-$HT_4$

ABSTRACT

In this work, we exemplified the "copride" family of drug candidates able to both inhibit acetylcholinesterase and to activate 5-$HT_4$ receptors, with anti-amnesiant and promnesiant activities in mice. Twenty-one analogs of donecopride, the first-in class representative of the series, were synthesized exploring the influence on the biological activities of the substituents (methoxy, amine and chlorine) carried by its phenyl ring. This work was the support of an intensive structure-activity relationship study and allowed to obtain some interesting derivatives of donecopride. In this respect, the replacement of the methoxy group of the latter with a deuterated one led to deudonecopride. On the other hand, the replacement of the chlorine atom of donecopride by various halogen atoms was of particular interest, among which fluorine led to a potent analog, we called flucopride. The latter exhibited promising *in vitro* activities associated to excellent drugability parameters. Flucopride was consequently involved in *in vivo* studies such as a scopolamine-induced deficit model of working memory and in a novel object recognition test. Through these evaluations, flucopride demonstrated both its antiamnesiant and promnesiant capacities, which could make it a potential preclinical drug candidate for the treatment of Alzheimer's disease.

## 1. Introduction

Alzheimer's disease (AD), the most preeminent form of dementia in the world, was, not long ago, still considered as a therapeutic impasse [1]. The marketed drugs, till now, mainly targeted acetylcholinesterase (AChE) in order to maintain longer the cholinergic neurotransmission and to alleviate the cognitive disorders accompanying the disease. These medicines, however, acted as purely symptomatic drugs, targeting exclusively the consequences of the neurodegeneration and, further, were doomed to lose their relative efficiency along the evolution of the disease. Concerning this time not only the consequences, but also the molecular causes of AD, three of the latter were the object, in the past twenty years, of a considerable amount of works, aiming at discovering novel drugs fighting them, namely the amyloid, tau and neuroinflammation hypotheses. Despite this unprecedented effort, no evidence came to corroborate these avenues until, recently, several antibodies targeting the amyloid aggregates appeared to display a relative therapeutic benefit against AD and consequently were approved

* Corresponding author.
** Corresponding author.
*E-mail addresses:* christophe.rochais@unicaen.fr (C. Rochais), patrick.dallemagne@unicaen.fr (P. Dallemagne).
[1] Present address: CRBM, CNRS UMR5237, F-34293 Montpellier cedex 5, France.

https://doi.org/10.1016/j.ejmech.2024.116975
Received 20 September 2024; Received in revised form 15 October 2024; Accepted 15 October 2024
Available online 18 October 2024

by Food and Drug Administration (FDA) [2]. Even if, the first of them, aducanumab (ADULHEM®) was the subject of a strong controversy [3,4], the results of the phase III clinical trials of the other ones, lecanemab (LEQEMBI®) [5] and donanemab [6–8], appear as able to correlate the decrease of the amyloid load, they are responsible for, and a relative improvement in cognitive performances of patients. Despite their drawbacks -most notably their Amyloid Related Imaging Abnormalities (ARIA)-type side effects and their high cost-, these antibodies seem to confirm the amyloid hypothesis as a valuable target. This could renew hopes of beating AD or most modestly slowing its progression, even with small molecules. The latter, indeed, can be considered as valuable alternative to antibodies, cheaper, able to penetrate in the brain through oral administration, more clinically efficient and potentially safer. Such a challenging goal, indeed, could be reached and specially, according to us, with pleiotropic drugs targeting not only the amyloid toxicity and/or load, but also the hyperphosphorylated protein Tau and the neuro-inflammation, AD patients are suffering from.

Among the possible drug candidates, perhaps able to exert these complementary effects in AD, we previously described donecopride as a promising Swiss-army knife, Multi Target-Directed Ligand (MTDL) exerting both AChE inhibitory and 5-$HT_4$ receptor agonist activities (Fig. 1) [9–11]. The latter is currently in regulatory preclinical trials and was also the subject of an intensive medicinal chemistry work, in order to achieve its declination into various derivatives, even perhaps more clinically relevant. The present work wishes to report the synthesis of various donecopride's derivatives, describing for the first time some modulations of the aromatic moiety (Fig. 1), as well as their *in vitro* and *in vivo* evaluation as potential novel drug candidates in AD therapy.

## 2. Results

### 2.1. Chemistry

Analogs of donecopride (**4a-m**) were obtained according to a multi-step sequence we previously described starting from benzoic acid **1a-k** (Scheme 1) [10]. The carboxylic acid group of the latter was activated with carbonyldiimidazole then converted into a α-ketoester group using potassium ethylmalonate. The resulting compounds **2a-k** were then involved in a nucleophilic substitution using *N*-Boc 4-(iodomethyl) piperidine. A saponification-decarboxylation sequence then yielded **3a-k**. Finally, TFA-*N*-deprotection of the latter, followed by the installation of a methylcyclohexyl moiety, gave the expected compounds **4a-k**. Further, debenzylation of **4i,j**, using HBr in AcOH or hydrogenolysis, yielded also **4l,m**.

The starting materials **1a-k** were commercially purchased, except **1a**, synthesized in two steps from 4-amino-2,5-difluorobenzonitrile, **1b, c**, which were obtained through regioselective halogenation of **1k** using NBS and NIS respectively, **1d,e**, resulting from the O-alkylation of 4-aminosalicylic acid, and **1i,j** which resulted from the *O*-benzylation of **1l,m** respectively (Scheme 2).

The halogeno analogs **4n,o** were obtained from **4a** named flucopride (Scheme 3), whose fumarate salt was also synthesized in view to be tested according to *in vivo* experiments.

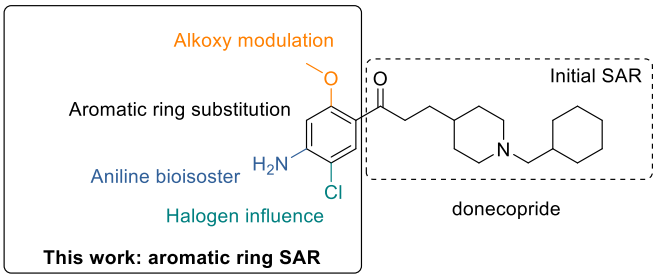


**Fig. 1.** Structure of donecopride and SAR exploration.

On the other hand, the iodo derivatives **4p,q** were obtained according to a more convergent sequence starting from the final compounds **4d,e** respectively, rather than from iodobenzoic acids as for **4c** which was obtained from **1c** (Scheme 4).

Finally, some novel derivatives of donecopride were synthesized starting from the latter as exemplified with the acetamido compounds **4r,s** or the desmethyldonecopride **4t** (Scheme 5). The latter was further engaged in several nucleophilic substitutions leading to the ethoxy- and fluoroethoxy derivatives **4u,v** as well as the deudonecopride **4w**.

### 2.2. In vitro results

#### 2.2.1. Binding to 5-$HT_4$ receptors and inhibition of cholinesterases

Twenty-two analogs of donecopride (*ie* all the synthesized compounds **4a-w**, except the *O*-benzyl compounds **4i,j**) were evaluated *in vitro* for their inhibitory activity towards (*h*)AChE and affinity towards (*h*)5-$HT_4$R (Table 1). Donecopride was used as a reference compound.

Among the tested compounds, six exhibited excellent inhibitory activities towards AChE ($IC_{50} \leq 60$ nM): **4a,h,k,r,s,w**, in comparison to donecopride ($IC_{50} = 16$ nM). The most inhibitory derivatives are the fluoro analog of donecopride (**4a**) ($IC_{50} = 24$ nM), named flucopride, the dechlorodonecopride (**4k**) ($IC_{50} = 26$ nM), the acetyldonecopride (**4r**) ($IC_{50} = 34$ nM) and the deudonecopride (**4w**) ($IC_{50} = 23$ nM). As expected, the fumarate salt of flucopride retains the inhibitory activity towards AChE ($IC_{50} = 29$ nM). Concerning the affinity towards 5-$HT_4$R, twelve of the twenty-two compounds displayed good affinity values with inhibition % at $10^{-8}$ M–30 %, but among the latter, only two showed impressive pleiotropic activities: flucopride (**4a**, $K_i = 10$ nM) and deudonecopride (**4w**, $K_i = 21$ nM). The fumarate salt of flucopride, again, kept the affinity of its base **4a** towards 5-$HT_4$R ($K_i = 16$ nM).

On the basis of its potent and balanced activities towards both AChE and 5-$HT_4$R, flucopride (**4a**) was selected for further *in vitro* investigations. Flucopride was found to be a partial 5-$HT_4$R agonist (67 %, Table 2 and Fig. 2A). Its selectivity for AChE versus butyrylcholinesterase (BuChE) was then established (Table 2). Flucopride was found to be 250 times more potent for AChE ($IC_{50} = 24$ nM) than for (*eq*) BuChE ($IC_{50} = 6.2$ μM) inhibition. Flucopride, further, interacts with the Peripheral Anionic Site (PAS) of (*ee*)AChE as attested by the displacement of propidium iodide from this site (22 % inhibition of the fluorescence of propidium bound to AChE at $10^{-5}$ M), accounting for a potential AChE-dependent amyloid aggregation inhibition in a similar manner as donepezil. This result is consistent with the mixed-type competitive AChE inhibitor profile of flucopride as established with the measure of the Lineweaver Burk plots of its inhibition kinetics (Fig. 2B).

#### 2.2.2. Promotion of the soluble amyloid protein precursor α (sAPPα) secretion in an in vitro cellular model

Flucopride was tested for its ability to promote the non-amyloidogenic processing of APP in COS-7 transiently expressing (*h*)5-$HT_4$ receptors [12,13]. In this model, flucopride behaved as a partial agonist, able to induce a dose-dependent sAPPα release with an $EC_{50}$ of 23.0 ± 9.9 nM and an $E_{Max}$ of 19.7 ± 0.6 % similar to RS 67333, a reference (*h*)5-$HT_4$R agonist ($EC_{50} = 40.0 \pm 17.9$ nM; $E_{Max} = 23.5 \pm 3.1$ %) (Fig. 3).

#### 2.2.3. Drugability parameters

Concerning its drugability parameters, flucopride exhibited good gastrointestinal track (GIT) penetration, whatever the pH values, and blood-brain barrier (BBB) cross-membrane penetration according to a Parallel Artificial Membrane Permeability Assay (PAMPA) and considering the logPe values obtained (Pe = PAMPA effective permeability coefficient) (Table 3).

The thermodynamic water solubility of flucopride was determined at various pH levels according to the classic shake-flask method and miniaturized UV spectrometric quantification (Table 3). Flucopride base

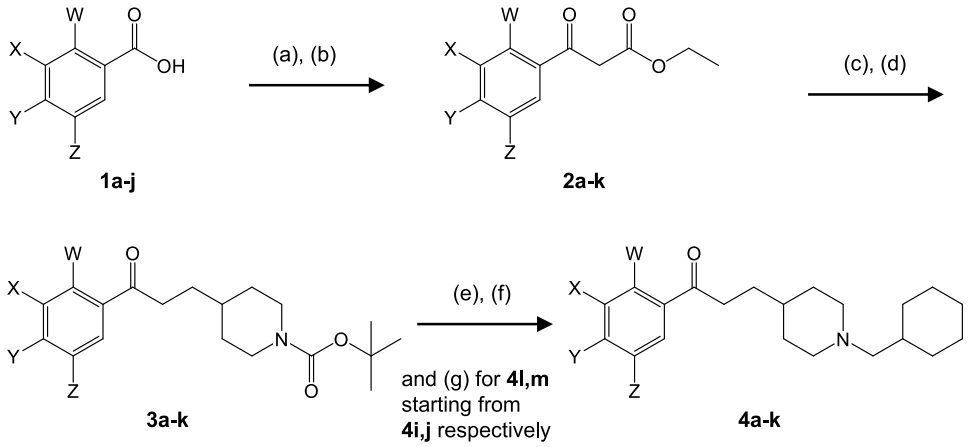


| cmpd | W | X | Y | Z |
|---|---|---|---|---|
| **a** | OMe | H | $NH_2$ | F |
| **b** | OMe | H | $NH_2$ | Br |
| **c** | OMe | H | $NH_2$ | I |
| **d** | OEt | H | $NH_2$ | H |
| **e** | $O(CH_2)_2F$ | H | $NH_2$ | H |
| **f** | H | H | $NH_2$ | H |
| **g** | OMe | H | H | H |
| **h** | H | H | $NH_2$ | Cl |
| **i** | H | H | OBn | H |
| **j** | OMe | H | OBn | Cl |
| **k** | OMe | H | $NH_2$ | H |
| **l** | H | H | OH | H |
| **m** | OMe | H | OH | Cl |

**Scheme 1.** Synthetic pathways for access to compounds **4a-m**. Conditions and reagents: (a) CDI, THF; (b) $KO_2CCH_2CO_2Et$, $MgCl_2$, THF; (c) *N*-Boc 4-iodomethylpiperidine, $K_2CO_3$, DMF; (d) KOH, EtOH/$H_2O$ reflux; (e) TFA, DCM; (f) (Bromomethyl)cyclohexane, $K_2CO_3$, DMF 110 °C; (g) HBr 33 %, AcOH, rt for **4l**; $H_2$, Pd/C, MeOH, rt for **4m.**

appears highly soluble in water. On the other hand, the ability of flucopride to inhibit the P-glycoprotein (P-gp)-mediated efflux of rhodamine123 was also evaluated on NCI/ADR-res cells at 1 and 10 μM. The inhibition at theses doses (125 and 111 % respectively) occurred into a lesser extent in comparison to cyclosporin at 50 μM which strongly inhibited rhodamine123 efflux through P-gp inhibition (400 %) (Table 3). Finally, flucopride was found not cytotoxic towards MRC5 cells, nor mutagenic in the AMES test.

### 2.2.4. *In vitro pharmacokinetic parameters for flucopride fumarate*

Taking into consideration the good drugability of flucopride, the *in vitro* pharmacokinetic parameters of its fumarate salt were evaluated.

*2.2.4.1. Metabolism. In vitro* metabolism of flucopride fumarate was investigated using incubations with human, dog, mouse and rat liver microsomes for 60 min. The collected samples were analyzed using a UPLC/QE-orbitrap-MS method developed for the purpose to monitor disappearance of the parent compound and to identify metabolites and to form metabolite profiles.

*2.2.4.2. Metabolic turnover in microsomes.* Relative LC/MS peak areas (%, in comparison to 0 min) observed after 0–60 min incubation with liver microsomes are shown in Table 4.

*2.2.4.3. Clearance calculations and in vivo extrapolation.* The results of the pharmacokinetic calculations are shown in Table 5 (without plasma protein binding correction).

The obtained half-life for flucopride fumarate in human liver microsomes was higher (59 min) than in dog, mouse and especially rat (half-lives 34, 20 and 6 min, respectively). The corresponding *in vitro* clearances were 11.7 μL/min/mg in human, 20.6 μL/min/mg in dog, 33.9 μL/min/mg in mouse and 116 μL/min/mg in rat. The predicted hepatic extraction ratio in human (without plasma protein binding correction) was 32 %, suggesting intermediate (close to low) hepatic clearance. In dog hepatic extraction ratio was 56 % and in mouse 42 %, suggesting intermediate hepatic clearance. In rat, hepatic extraction ratio was 75 %, suggesting high hepatic clearance.

*2.2.4.4. Metabolite identification and metabolite profiles.* In total, twenty-

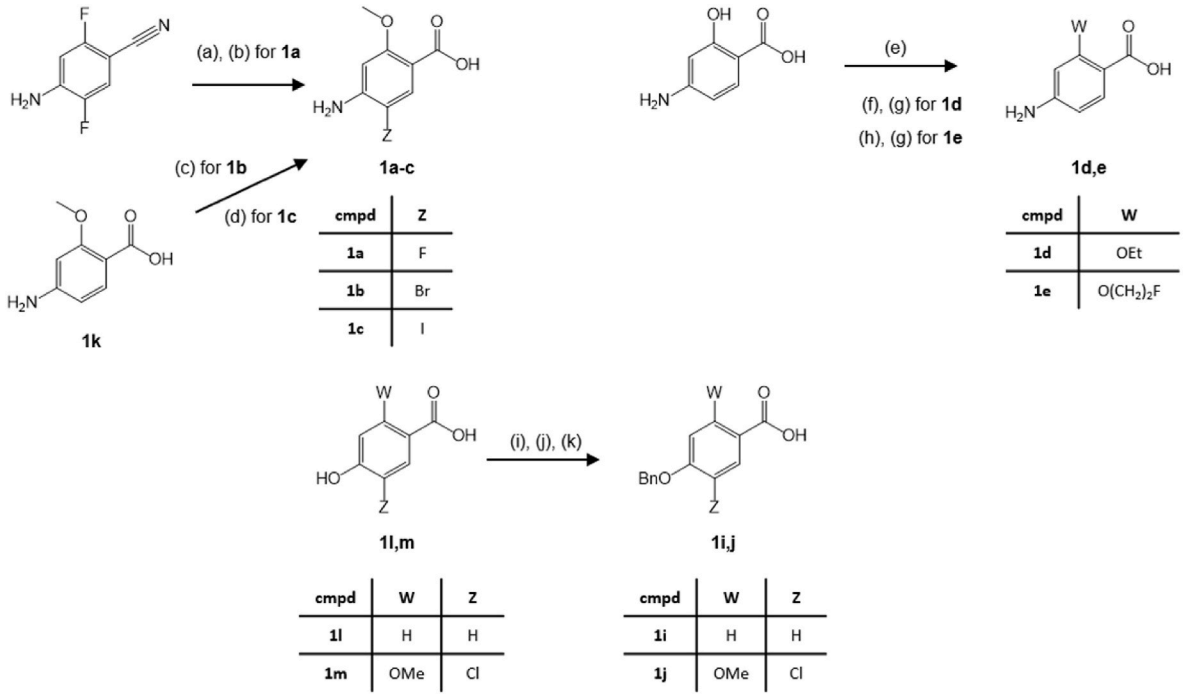


| cmpd | Z |
|---|---|
| 1a | F |
| 1b | Br |
| 1c | I |

| cmpd | W |
|---|---|
| 1d | OEt |
| 1e | $O(CH_2)_2F$ |

| cmpd | W | Z |
|---|---|---|
| 1l | H | H |
| 1m | OMe | Cl |

| cmpd | W | Z |
|---|---|---|
| 1i | H | H |
| 1j | OMe | Cl |

**Scheme 2.** Synthetic pathways for access to compounds **1a-e,i,j**. Conditions and reagents: (a) *t*-BuOK, MeOH, dry THF, rt; (b) KOH, EtOH/$H_2O$ reflux; (c) NBS, dioxane, rt; (d) NIS, dioxane, rt; (e) $H_2SO_4$, MeOH, reflux; (f) EtI, $K_2CO_3$, DMF, 70 °C; (g) NaOH 1 N, EtOH, rt; (h) $F(CH_2)_2OTs$, $K_2CO_3$, DMF, 70 °C; (i) $SOCl_2$, MeOH, reflux; (j) BnBr, $K_2CO_3$, DMF, rt; (k) NaOH 1 N, EtOH, rt.

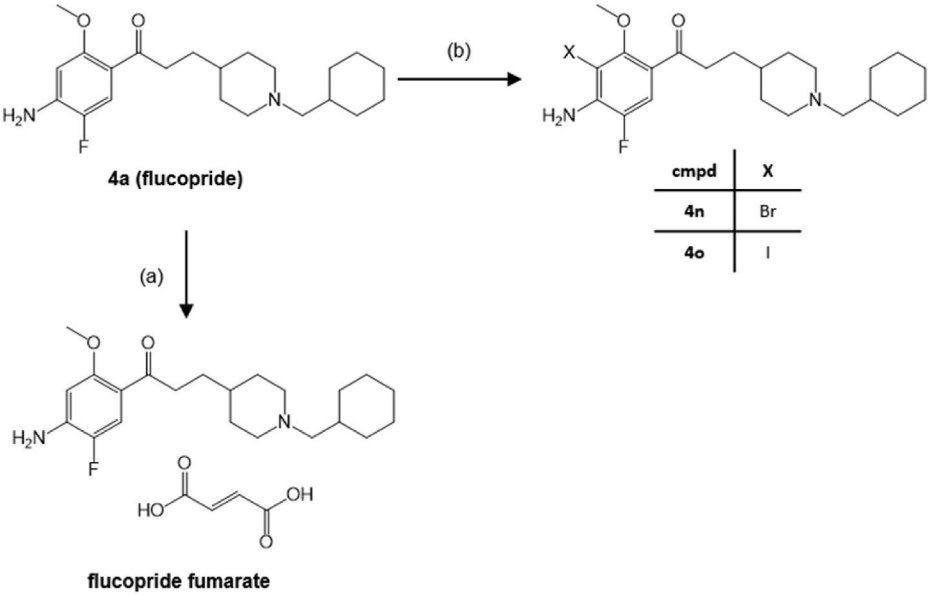


| cmpd | X |
|---|---|
| 4n | Br |
| 4o | I |

**Scheme 3.** Synthetic pathways for access to compounds **4n,o** and the fumarate salt of flucopride. Conditions and reagents: (a) fumaric acid, iPrOH, reflux (b) NBS, AcOH, rt; for **4n**; NIS, AcOH, rt for **4o**.

nine metabolites were observed for flucopride fumarate and from incubations with human, dog, mouse and rat liver microsomes. Seventeen metabolites were observed in human, hydroxylation in cyclohexane being clearly the main metabolite with 22 % share of the total LC/MS peak area at 60 min time point (*vs* 67 % for flucopride fumarate). The next most abundant metabolites resulted from hydroxylations in methylcyclohexane, ketone formation in ethylpiperidine + aromatic N-oxidation, and dealkylation by loss of methylcyclohexane, each with about 1–3 % shares of the total related peak area. Metabolites specific to human only were not observed. All above mentioned most abundant human metabolites were observed in all investigated species, although their relative abundances were variable.

*2.2.4.5. CYP inhibition.* The inhibition potential of flucopride fumarate towards major drug-metabolizing CYP enzymes was studied in human liver microsomes (Table 6). The inhibition potential towards CYP1A2, CYP2A6, CYP2B6, CYP2C8, CYP2C9, CYP2C19, CYP2D6 and CYP3A4 was assessed using CYP specific probe reactions in cocktail incubation.

Incubations with flucopride fumarate indicated inhibition towards CYP1A2, CYP2B6, CYP2C19, CYP2D6 and CYP3A4 and potentially

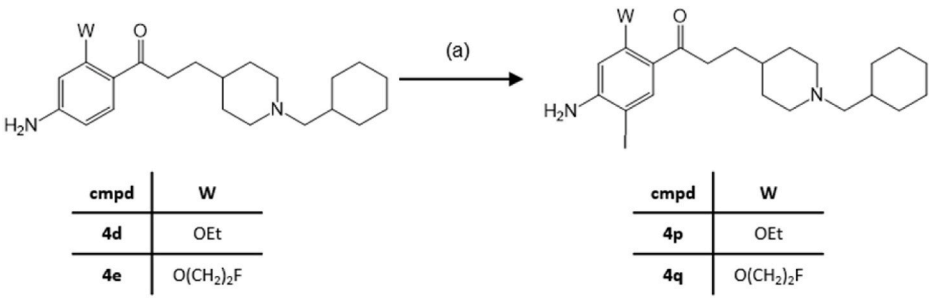


**Scheme 4.** Synthetic pathways for access to compounds **4p,q**. Conditions and reagents: (a) NaI, $AcOH/H_2O_2$ 30 % (2/1), rt.

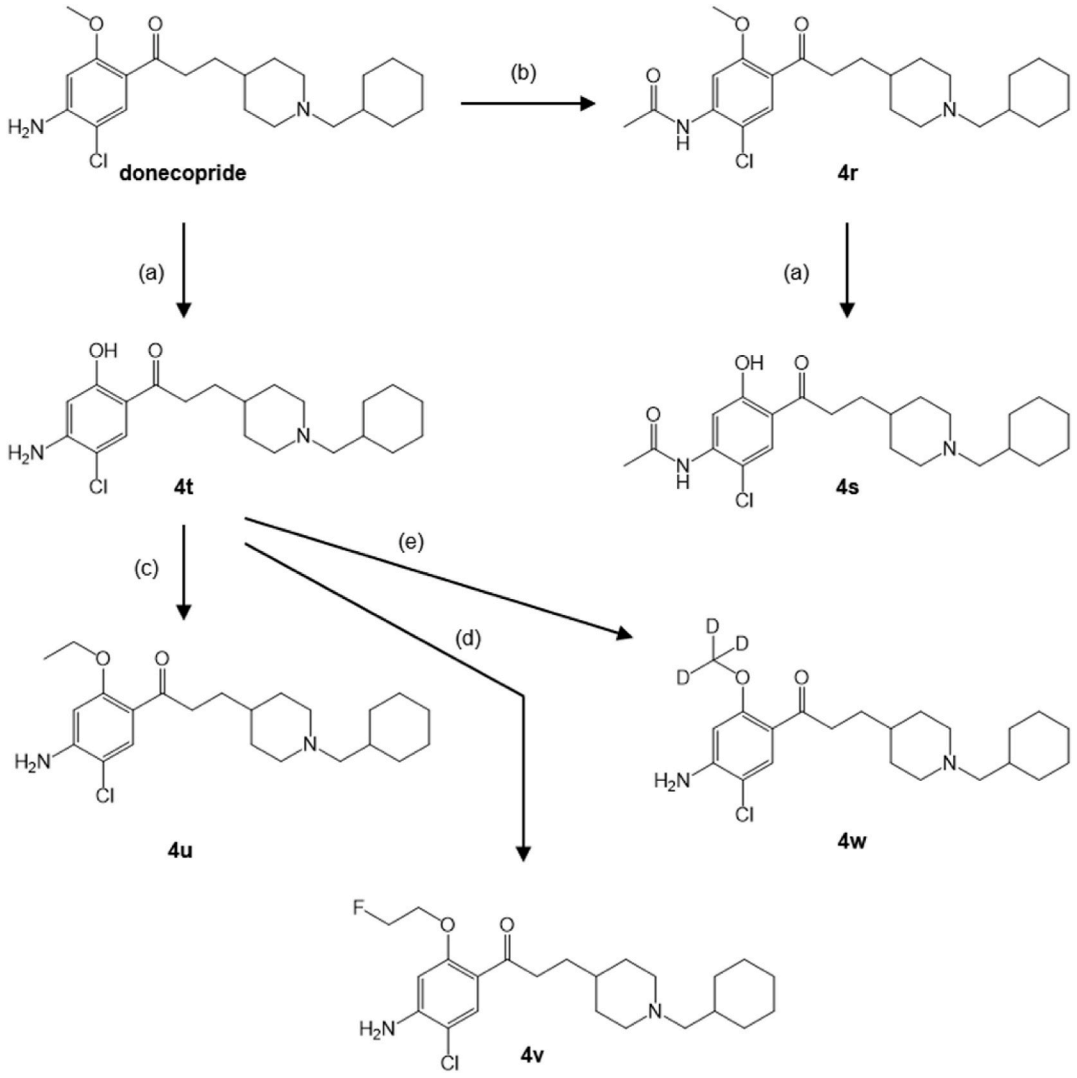


**Scheme 5.** Synthetic pathways for access to compounds **4r-w**. Conditions and reagents: (a) $BBr_3$, DCM; (b) $Ac_2O$; (c) EtI, $K_2CO_3$, DMF, 110 °C; (d) 2-fluoroethyl 4-methylbenzenesulfonate, $K_2CO_3$, DMF, 110 °C; (e) $CD_3I$, $K_2CO_3$, DMF.

towards CYP2C8 and CYP2C9. Inhibition towards CYP2D6 was the most potent with $IC_{50}$ of 0.6 μM followed by inhibition towards CYP2C19 ($IC_{50}$ 7.2–12.1 μM depending on the probe reaction) and CYP3A4 ($IC_{50}$ 3.5–18.5 μM depending on the probe reaction). The data did not indicate strong inhibition towards CYP2A6 at the concentration range tested (0.01–100 μM).

### 2.3. In vivo results

After preliminary pharmacokinetic and toxicology studies, flucopride was investigated in two animal models of AD.

#### 2.3.1. Preliminary pharmacokinetic study of flucopride

Pharmacokinetics study was performed in mouse and rat (respectively, C57Bl6 and Wistar strain). Flucopride was administered intravenously (0.3, 1, 3 mg/kg, iv.), orally (1, 3, 9 mg/kg, po.) and

**Table 1**
(*h*)AChE inhibitory activity and (*h*)5-HT$_4$R affinity for donecopride and compounds **4a-w**.

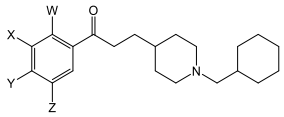


| Compd | W | X | Y | Z | (*h*)AChE | | (*h*)5HT$_4$R | | |
|---|---|---|---|---|---|---|---|---|---|
| | | | | | %inh | $IC_{50}$ (nM) n = 2 | %inh $10^{-6}$M | %inh $10^{-8}$M | $K_i$ (nM) n = 3 |
| *Donecopride*[a] | *OMe* | *H* | *$NH_2$* | *Cl* | *96 % 10$^{-5}$M* | *16 ± 5* | *101 %* | *73 %* | *10.04 ± 0.9* |
| **4a** (flucopride) | OMe | H | $NH_2$ | F | 96 % $10^{-6}$M | 24 ±0.2 | 100 % | 66 % | 9.6 ±3.0 |
| flucopride fumarate | OMe | H | $NH_2$ | F | 96 % $10^{-6}$M | 29 ±0.2 | 102 % | 68 % | 16.3 ±3.1 |
| **4b** | OMe | H | $NH_2$ | Br | 98 % $10^{-5}$M | 99 ±26 | 105 % | 61 % | ND |
| **4c** | OMe | H | $NH_2$ | I | 88 % $10^{-5}$M | 304 ±53 | 103 % | 36 % | ND |
| **4d** | OEt | H | $NH_2$ | H | 93 % $10^{-6}$M | 87.1 ± 18.6 | 101 % | 38 % | 24.7 ± 5.3 |
| **4e** | $OCH_2CH_2F$ | H | $NH_2$ | H | 79 % $10^{-6}$M | 318.3 ±12.8 | 100 % | 27 % | 39.9 ±4.9 |
| **4f** | H | H | $NH_2$ | H | 78 % $10^{-6}$M | 316.6 ±115.8 | 80 % | 4 % | ND |
| **4g** | OMe | H | H | H | 85 % $10^{-6}$M | 166 ±3.9 | 102 % | 31 % | 120.8 ±62.8 |
| **4h** | H | H | $NH_2$ | Cl | 96 % $10^{-6}$M | 49.7 ±2.9 | 97 % | 10 % | ND |
| **4k** | OMe | H | $NH_2$ | H | 97 % $10^{-5}$M | 26 ±14 | 96 % | 10 % | ND |
| **4l** | H | H | OH | H | 35 % $10^{-6}$M | – | 102 % | 58 % | 17.6 ±3.8 |
| **4m** | OMe | H | OH | Cl | 78 % $10^{-6}$M | 301 ±1 | 76 % | 2 % | ND |
| **4n** | OMe | Br | $NH_2$ | F | 85 % $10^{-6}$M | 308.9 ±31.9 | 80 % | 8 % | ND |
| **4o** | OMe | I | $NH_2$ | F | 89 % $10^{-6}$M | 233.9 ±35.3 | 89 % | 2 % | ND |
| **4p** | OEt | H | $NH_2$ | I | 51 % $10^{-6}$M | – | 103 % | 65 % | 86 ±19.4 |
| **4q** | $OCH_2CH_2F$ | H | $NH_2$ | I | 45 % $10^{-6}$M | – | 101 % | 22 % | 521 ±261 |
| **4r** | OMe | H | NHAc | Cl | 98 % $10^{-6}$M | 34 ±5 | 94 % | 1 % | 270 ±134 |
| **4s** | OH | H | NHAc | Cl | 94 % $10^{-6}$M | 57.3 ±6.7 | 47 % | 8 % | ND |
| **4t** | OH | H | $NH_2$ | Cl | 93 % $10^{-5}$M | 411 ±11 | 96 % | 3 % | ND |
| **4u** | OEt | H | $NH_2$ | Cl | 69 % $10^{-6}$M | 395 ±4 | 103 % | 86 % | ND |
| **4v** | $OCH_2CH_2F$ | H | $NH_2$ | Cl | 60 % $10^{-6}$M | 625 ±33 | 102 % | 78 % | ND |
| **4w** (deu-donecopride) | $OCD_3$ | H | $NH_2$ | Cl | 92 % $10^{-6}$M | 22.6 ±3.8 | 98 % | 29 % | 20.8 ±3.7 |

[a] Results reported from Lecoutey et al. [9].

**Table 2**
(*eq*)BuChE inhibitory activity, (*ee*)AChE propidium iodide displacement inhibition and (*h*)5-HT$_4$R pharmacological profile for flucopride.

| (*eq*)BuChE | | (*ee*)AChE | (*h*)5-HT$_4$R | |
|---|---|---|---|---|
| %inh $10^{-5}$M | $IC_{50}$ (nM) n = 2 | Propidium iodide displacement (% inhibition at $10^{-5}$M) | cAMP | |
| | | | % of serotonin max. response n = 3 | $EC_{50}$ (nM) n = 3 |
| 65 % | 6200 | 22 | 67.3 ± 5.1 | 1.3 ± 0.2 |

intraperitoneally (0.3, 1, 3 mg/kg, ip.). Each dose was tested in three animals. The study was performed using a terminal blood sampling method conducted under anesthesia at six different time points. CSF sampling was performed only after i.p. administration. It was then possible to evaluate pharmacokinetic parameters, oral bioavailability and cerebrospinal fluid entry using a non-compartmental analysis (NCA) (Fig. 4).

Plasma concentrations of flucopride were higher than the limit of quantification and pharmacokinetic parameters have been calculated, except in rats dosed at 0.3 and 1 mg/kg ip. and po. respectively (data not shown).

By intravenous (iv.) administration, flucopride fumarate exhibited a moderate plasma clearance in mice and rats, ranging from 2.13 to 5.28 L/h/kg, with an exception in mice at 3 mg/kg, where it was higher at

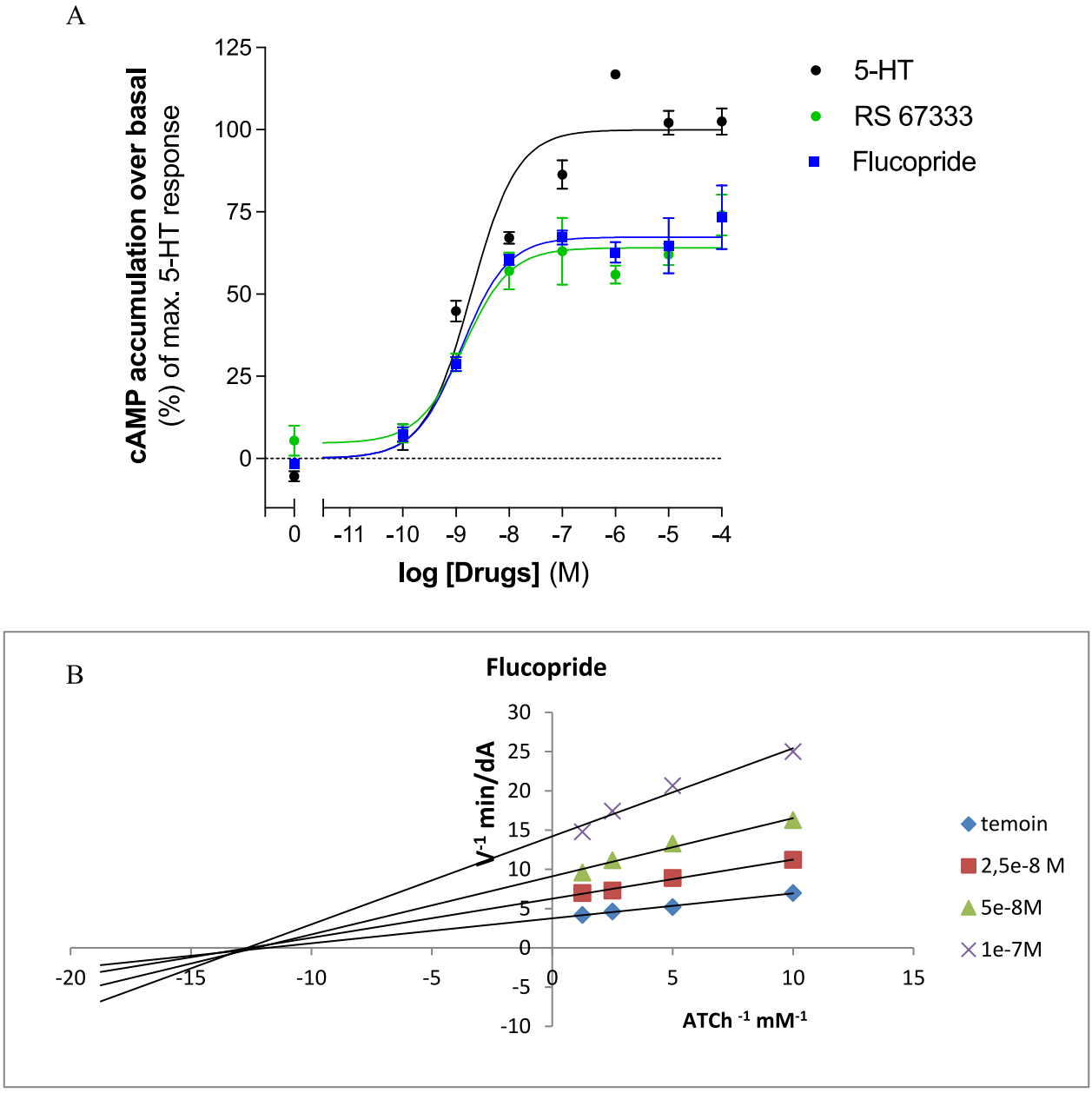


**Fig. 2. A)** cAMP accumulation upon (*h*)5-HT$_4$R activation by flucopride. **B)** Lineweaver Burk plots of inhibition kinetics of flucopride. 5-HT: serotonin, full agonist; RS 67333: reference partial agonist.

11.48 L/h/kg. The volume of distribution showed a wide range, spanning from 3.6 to 13.2 L/kg. Half-lives ($T_{1/2}$) and mean residence times (MRT) were relatively short in both species across all three doses: 0.796–1.123 h and 1.15–1.70 h, in mice and rats, respectively.

Upon oral administration, flucopride was detected in the plasma of both mice and rats. The absolute bioavailability (F) was calculated using data from the iv. route, yielding values that were highly varied and dose-dependent. This variability may be attributed to the non-linear relationship observed between Area Under The Curve (AUC) and dose for both iv. and oral routes under our experimental conditions. In mice, oral bioavailability ranged from low to good (12.4 %–75.3 %), while in rats, the oral bioavailability of flucopride appeared to be lower (3.6 %–9.0 %).

To assess central nervous system uptake, flucopride concentration was measured in cerebrospinal fluid (CSF) following intraperitoneal (ip.) administration at doses of 0.3, 1 and 3 mg/kg (Fig. 5). Concentration in CSF ($C_{CSF}$) can serve as a surrogate for the interstitial fluid ($C_{ISF}$) in rodents, assuming rapid equilibration between the ISF and CSF compartments across the ependymal layer. Due to low protein concentrations, $C_{CSF}$ may be equivalent to the unbound drug concentration in the CSF [14]. In our experimental conditions, flucopride was only detectable in CSF at the highest dose. At 3 mg/kg, the AUCs were 7.66 ± 0.41 in mice and 9.26 ± 1.12 ng/mL.h in rats respectively.

### 2.3.2. *Pharmacological and toxicological properties of flucopride*

To assess the working doses ranging, the toxicological profile of flucopride fumarate was investigated and compared to hyper- and hypo-active reference drugs. Two doses of flucopride fumarate were tested −100 mg/kg and a 10-fold weaker dose. Adverse effect was revealed only after administration of the highest dose.

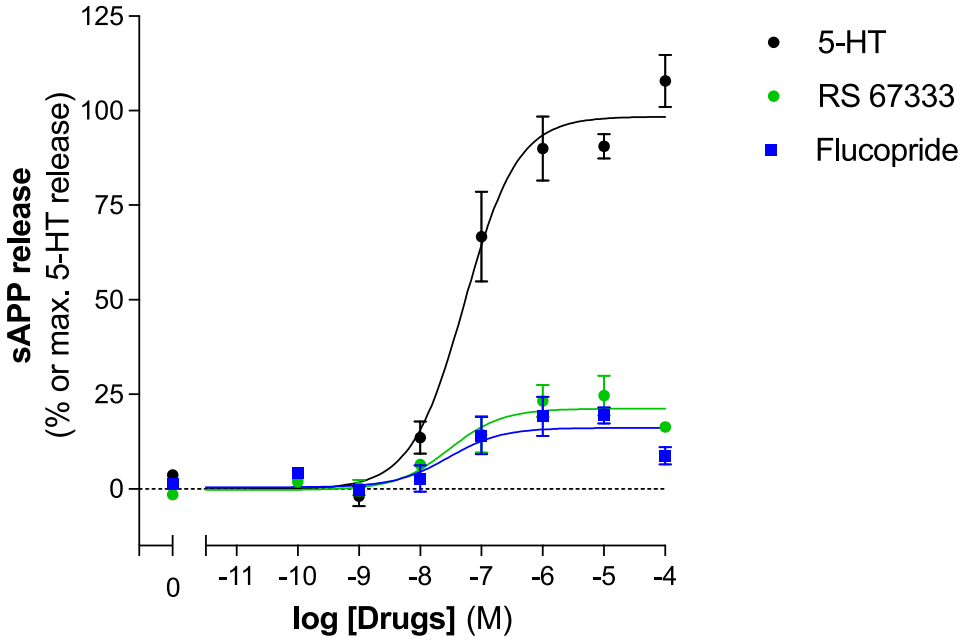


**Fig. 3.** Promotion of non-amyloidogenic APP cleavage by flucopride in COS-7 cells transiently expressing (*h*)5-HT$_4$ receptors (Data are expressed as the mean SD, n = 2). 5-HT: serotonin, full agonist; RS 67333: reference partial agonist.

**Table 3**
Drugability parameters for flucopride (**4a**).

| | | | |
|---|---|---|---|
| PAMPA (logPe) | GIT | pH 7.4 | −4.08 ± 0.04 |
| | | pH 6 | −4.19 ± 0.01 |
| | | pH 5 | −4.23 ± 0.04 |
| | BBB | | −4.39 ± 0.04 |
| Solubility in water (μM) | $S_{int}$ (pH 12) | | 2.0 ± 1.3 |
| | $S_{physio}$ (pH 7.4) | | 104.0 ± 7.7 |
| | $S_w$ (Water) | | 444.2 ± 75.8 |
| P-gp inhibition (%) | NCI/ADR-res | | 100 ± 23 |
| | Cyclosporine 50 μM | | 400 ± 134 |
| | **4a** 10 μM | | 111 ± 18 |
| | **4a** 1 μM | | 125 ± 32 |
| Cytotoxicity on MRC5 cell (% growth inhibition) | **4a** 10 μM | | 0 ± 14 |
| | **4a** 1 μM | | 0 ± 14 |
| AMES test | No mutagenicity | | |

*2.3.3. Effect of flucopride fumarate on spontaneous locomotor activity*

To quantify the hypoactivity effect of flucopride fumarate, it was tested in actimeter test at three doses from 10 mg/kg and with 10 and 100-fold lower doses. A significant decrease of spontaneous locomotor activity was revealed only at the highest tested dose (10 mg/kg) (Fig. 6). Therefore, to avoid any locomotor biased in the interpretation of the behavioral data, the dose range 0.3-1-3 mg/kg was chosen.

*2.3.4. Effect of flucopride fumarate on scopolamine-induced impairment during the spontaneous alternation test*

Next, the spontaneous alternation test was performed. Compared to control group, scopolamine treated animals displayed a memory deficit with an alternation percentage around 50 %. Administration of flucopride fumarate, only at the highest dose (3 mg/kg), reversed the scopolamine-induced spontaneous alternation deficit (Fig. 7). Of note, this anti-amnesic effect is also observable after administration of DPZ combined to RS.

*2.3.5. Effect of flucopride in novel object recognition test (NORT)*

The object recognition test was next used with a long interval inter-trial (72h) in order to observe a natural forgetting in the control group. As expected, control group did not discriminate the novel from the familiar object and displayed similar exploration time for both. When treated with flucopride fumarate, animals treated with the lowest dose (0.3 mg/kg) displayed significant recognition memory performances (Figs. 8 and 9). Interestingly, a comparable effect has been obtained with the association of RS to DPZ.

## 3. Discussion

This work was dedicated to a structure-activity relationships (SAR) study concerning the substituents in various positions of the phenyl ring in donecopride in view to improve, in novel compounds, the dual AChE inhibitory and 5-HT$_4$R agonist activities comparatively to those of the latter. As usually, with regard to dual compounds, the difficulty lied in the risk that enhancing one of the activities was detrimental to the other. In view to establish potentially useful SAR, we successively undertook the step-by-step substitution of the W, X, Y and Z substituents carried by the phenyl ring of donecopride.

The first pharmacomodulations which were undertaken, concerned the replacement of its OMe group by various substituents (**4h,t-w**) (Fig. 9). This position seems moderately involved in the inhibition of AChE since the activity was maintained or slightly decreased for the five resulting compounds. In contrast an alkoxy group in this position appears necessary to the 5-HT$_4$R affinity since removing the OMe group (**4h**) or replacing it by a OH group (**4t**) suppressed the activity. The latter was however maintained with W = OEt (**4u**), $OCH_2CH_2F$ (**4v**) and $OCD_3$ (**4w**). Concerning further modifications of some of these derivatives, the acetyl group in **4s** improved the AChE inhibition relatively to **4t**, but did not allow to recover the lost 5-HT$_4$ affinity. The loss of the chlorine atom in **4d** did not change the activities relatively to **4u**, but its replacement by an iodine atom (**4p**) was detrimental to both activities. The same pharmacomodulations applied to **4v** led to similar results for **4e** and **4q**. Finally, this first structure declination led to a unique sound dual compound, the deudonecopride (**4w**).

The amino group of donecopride appears essential for the 5-HT$_4$R

**Table 4**
Mean relative abundances (% to 0 min, n = 1) of flucopride fumarate in liver microsomes from the investigated species at each time point. Non-linear graph with values.

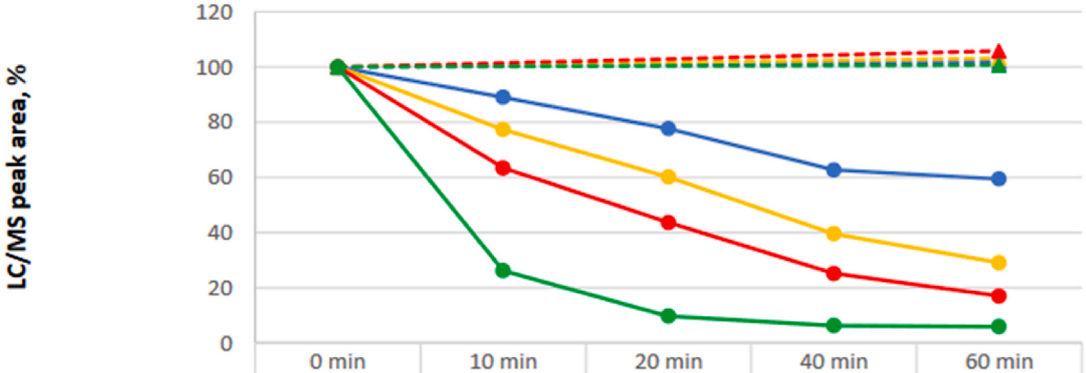


| | 0 min | 10 min | 20 min | 40 min | 60 min |
|---|---|---|---|---|---|
| Human | 100 | 89 | 78 | 63 | 59 |
| Human control | 100 | | | | 102 |
| Dog | 100 | 77 | 60 | 40 | 29 |
| Dog control | 100 | | | | 103 |
| Mouse | 100 | 63 | 44 | 25 | 17 |
| Mouse control | 100 | | | | 106 |
| Rat | 100 | 26 | 10 | 6 | 6 |
| Rat control | 100 | | | | 101 |

**Table 4**
Toxicological profile of flucopride fumarate.

| Compound | Doses (mg/kg) | Symptoms |
|---|---|---|
| Amphetamine | 2 | Hyperactivity<br>Exophtalmy, Irritability |
| Chlorpromazine | 10 | Hypoactivity<br>Ataxia, Sleep |
| Flucopride fumarate | 10 | No symptoms |
| | 100 | Hypoactivity<br>Passivity, Relaxation<br>Ptosis, Tremors<br>Convulsions |

**Table 5**
Kinetic *in vitro* calculations and extrapolation based on the disappearance data of flucopride fumarate in liver microsomes.

| | Human | Dog | Mouse | Rat |
|---|---|---|---|---|
| Half-life (min) | 59 | 34 | 20 | 6 |
| *In vitro* Clearance (µL/min/mg) | 11.7 | 20.6 | 33.9 | 116 |
| *In vivo* Clearance extrapolation (µL/min) | 460 | 173 | 1.01 | 12.6 |
| Hepatic extraction (%) | 32 | 56 | 42 | 75 |

affinity since its replacement by OH led to a loss of activity (**4m**) while its acetylation (**4r**) decreased it (Fig. 10). The AChE inhibitory activity seems less dependent from the amino group. The hydroxy analog of donecopride (**4m**) was found slightly less inhibitor while its acetyl derivative (**4r**) inhibited AChE in a similar manner as donecopride. The same goes for the acetyldealkoxy derivative (**4s**) which, as already seen, maintained its AChE activity but totally lost its 5-$HT_4$R affinity. Surprisingly, the simplified analog of **4m**, compound **4l**, is devoid of AChE inhibitory activity but recovered a significant 5-$HT_4$R affinity. No novel dual compound emerged from these pharmacomodulations.

The last structural pharmacomodulation of donecopride concerned its chlorine atom (Fig. 11). It appeared less implicated in the AChE

**Table 6**
Estimated $IC_{50}$ (µM) values for flucopride fumarate incubated with human liver microsomes.

| CYP | Substrate | Metabolite | $IC_{50}$ (µM) |
|---|---|---|---|
| CYP1A2 | Phenacetin | Acetaminophen | 83.1 |
| CYP2A6 | Coumarin | 7-OH-Coumarin | >100 |
| CYP2B6 | Bupropion | OH-Bupropion | 95.7 |
| CYP2C8 | Repaglinide | OH-Repaglinide | >100 |
| CYP2C9 | Diclofenac | 4′–OH–Diclofenac | >100 |
| CYP2C19 | Omeprazole | 5-OH-Omeprazole | 7.2 |
| | Omeprazole | Desmethylomeprazole | 12.1 |
| CYP2D6 | Dextromethorphan | Dextrorphan | 0.6 |
| CYP3A4 | Omeprazole | 3-OH-Omeprazole | 5.4 |
| | | Omeprazole sulphone | 3.5 |
| | Testosterone | 6β–OH–Testosterone | 8 |
| | Midazolam | 1′–OH–Midazolam | 23.1 |

activity since the latter was maintained with a hydrogen (**4k**) or a fluorine atom (**4a**) and slightly decreased with a bromine (**4b**) or iodine atom (**4c**). This Z substituent, however, seems more important for the 5-$HT_4$R affinity: The dechloro analog of donecopride totally lost the activity, while its fluoro (**4a**) and bromo (**4b**) analogs kept it. The iodo analog (**4c**) showed a decreased 5-$HT_4$R affinity. As already seen, the ethoxy (**4d**) and fluoroethoxy (**4e**) analogs of **4k** showed decreased AChE activities but recovered 5-$HT_4$R affinities. Finally, the most simplified methoxy analog (**4g**) partially recovered its 5-$HT_4$R affinity while the amino one (**4f**) did not.

As anticipated, the structural requirements for each of the two expected activities are sometimes contradictory. Two novel potent dual compounds, however, were thus identified: **4w**, we called deudonecopride, and **4a**, we called flucopride. Some other compounds, showed either dual less potent AChE and 5-$HT_4$R activities (**4c,g**) or relatively imbalanced activities (**4b,d,e,r,u,v**).

Since flucopride acts as a selective, dual binding site AChE inhibitor and as a potent partial 5-$HT_4$R agonist, able to promote the release *in*

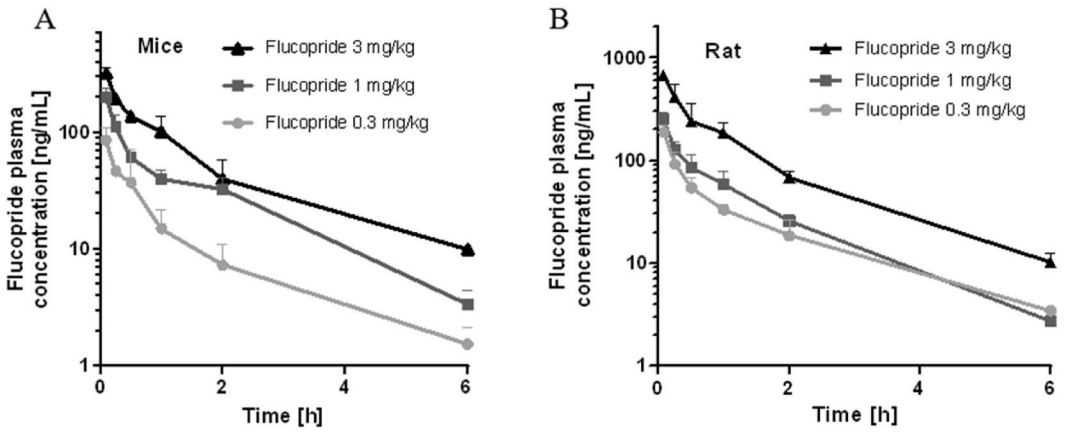


**Fig. 4.** Mean plasma concentration-time curves for flucopride in mice (A) and rats (B), after a single dose IV of 0.3, 1 or 3 mg/kg (n = 3/dose).

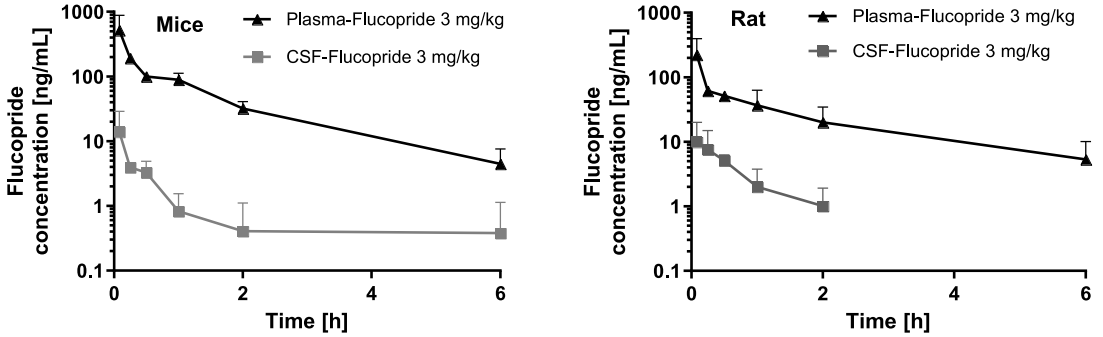


**Fig. 5.** Mean CSF and plasma concentration–time curves of flucopride after a single intraperitoneal dose of 3 mg/kg to male (A) mice (n = 3) or (B) rats (n = 3).

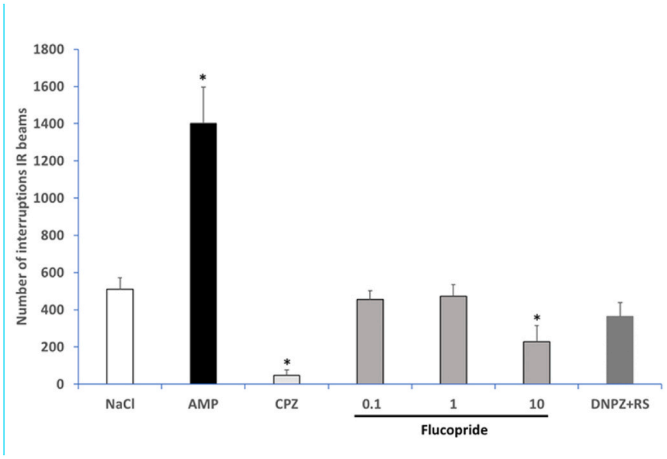


**Fig. 6.** Effect of flucopride fumarate on spontaneous locomotor activity. Data are expressed as the mean ± SEM (n = 9). Drugs were administered intraperitoneally 30 min before placing mice in the actimeter. Flucopride fumarate: 0.1–1–10 mg/kg; AMP: amphetamine 2 mg/kg; CPZ: chlorpromazine 10 mg/kg; DPZ (donepezil) + RS (RS 67333): 0.3 mg/kg + 0.1 mg/kg (*p < 0.05 versus NaCl group, SNK test).

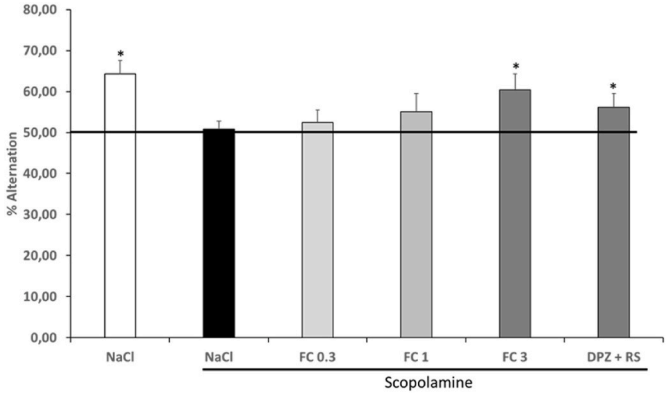


**Fig. 7.** Effect of flucopride fumarate on scopolamine-induced impairment during the spontaneous alternation test. Data are expressed as the mean ± SEM (n = 10). Drugs were administered ip. 30 min before the test, except scopolamine was administered subcutaneously (sc.) 20 min prior the test. FC (flucopride fumarate): 0.1, 0.3, 3 mg/kg; DPZ + RS: 0.3 mg/kg + 0.1 mg/kg; Scopolamine: 0.5 mg/kg (*p < 0.05 versus 50 %; univariate *t*-test).

*vitro* of sAPPα, with further good drugability and pharmacokinetic parameters, its fumarate salt was involved in an *in vivo* study at 0.3, 1 and 3 mg/kg in mice through intraperitoneal route. Flucopride fumarate exhibited an anti-amnesiant effect in a scopolamine-induced deficit model of working memory at 3 mg/kg. Flucopride fumarate, furthermore, demonstrated a promnesiant effect towards the recognition memory in a NORT at 0.3 mg/kg. The differences in active doses (0.3 mg/kg for novel object recognition test, 3 mg/kg for the spontaneous alternation test) can be attributed to the different conditions involved in the two tests: cholinergic hypofunction (spontaneous alternation) versus spontaneous forgetting in basal conditions (object recognition).

Concerning the object recognition test, we obtained results similar to those of donecopride [9]: procognitive effect at 0.3 and 1 mg/kg and no effect at 3 mg/kg. We therefore find with flucopride the same shape of

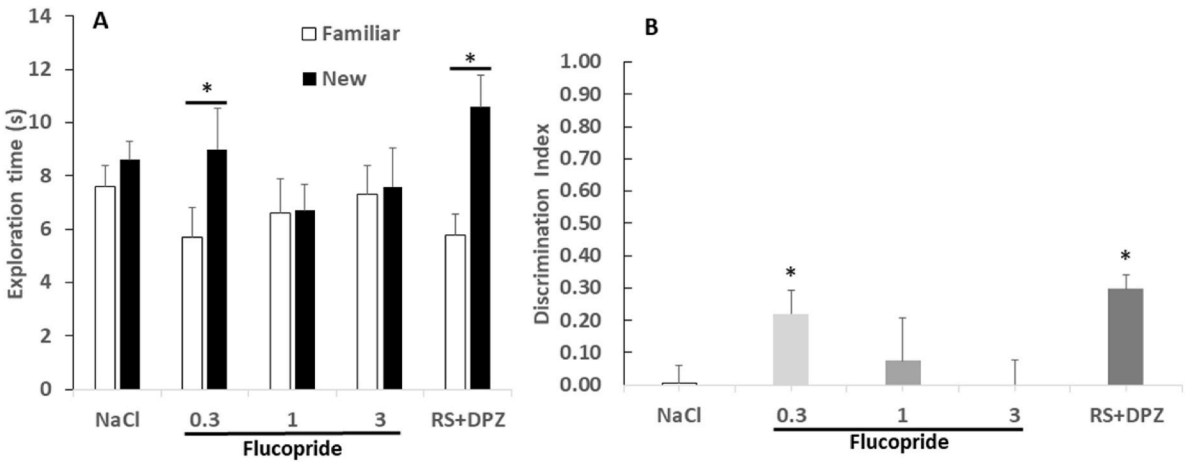


**Fig. 8.** (A): Effect of flucopride fumarate on memory recognition performances. Data (exploration times of familiar and novel object) are expressed as the mean ± SEM (n = 10). Drugs were administered ip. 30 min before the session 1 of test. FC (flucopride fumarate): 0.1, 0.3, 3 mg/kg; DPZ + RS: 0.3 mg/kg + 0.1 mg/kg (*p < 0.05; univariate *t*-test). (B): Effect of flucopride fumarate on memory recognition performances. Data (discrimination index) are expressed as the mean ± SEM (n = 10). Drugs were administered ip. 30 min before the session 1 of test. FC (flucopride fumarate): 0.1, 0.3, 3 mg/kg; DPZ + RS: 0.3 mg/kg + 0.1 mg/kg (*p < 0.05 versus 0 value; univariate *t*-test).

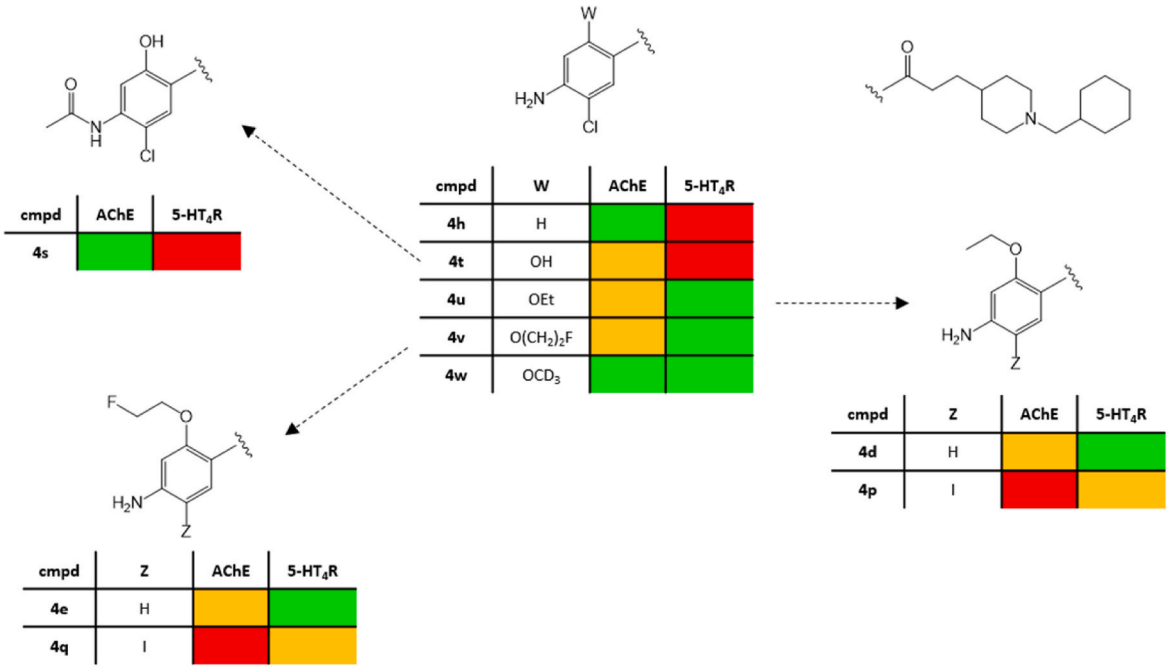


**Fig. 9.** Pharmacomodulations of donecopride: influence of the W substituent (green: activity enhanced or maintained; orange: activity slightly decreased; red: activity lost).

the inverted U dose-effect curve suggesting that the procognitive effect in basal conditions (no pharmacologically-induced deficit) depends closely on the level of stimulation of cholinergic transmission and that the optimal level would be obtained at low/moderate doses and would be exceeded at high doses.

Concerning the spontaneous alternation test, donecopride reversed the effect of scopolamine up to a dose of 3 mg/kg [10], a dose higher than that exerting a procognitive effect in the object recognition test in basal conditions. It therefore appears overall that for MTDLs such as donecopride and flucopride, the anti-amnesic doses (spontaneous alternation deficit induced by scopolamine) are greater than the procognitive doses (object recognition test in condition of natural forgetting).

Finally, we obtain a significant effect in both tests (both procognitive and anti-amnestic) with the association RS (0.1 mg/kg) + DPZ (0.3 mg/kg) suggesting that under these dosage conditions, we obtain an intermediate level of cholinergic stimulation allowing both to counterbalance the amnestic effects of scopolamine and to improve recognition memory performances in conditions of natural forgetting.

## 4. Conclusion

In conclusion, the present work confirmed the interest lying in dual compounds exhibiting both an AChE inhibitory and 5-$HT_4$R agonist activities. Useful pharmacomodulations of donecopride, the first-in-class representative of this new pharmacological family, yielded novel dual agents, such as flucopride, a fluoro analog of donecopride. Flucopride fumarate displayed both anti-amnesiant and promnesiant

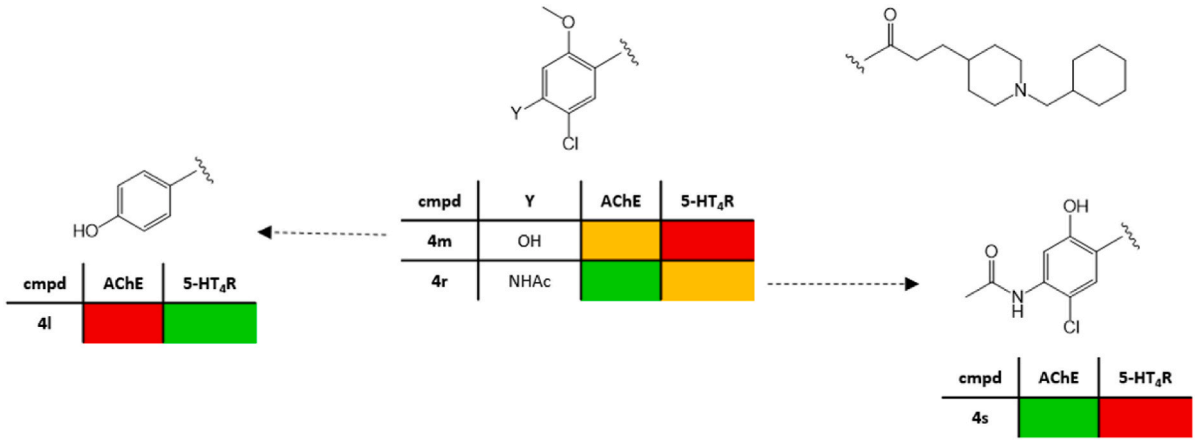


**Fig. 10.** Pharmacomodulations of donecopride: influence of the Y substituent (green: activity enhanced or maintained; orange: activity slightly decreased; red: activity lost).

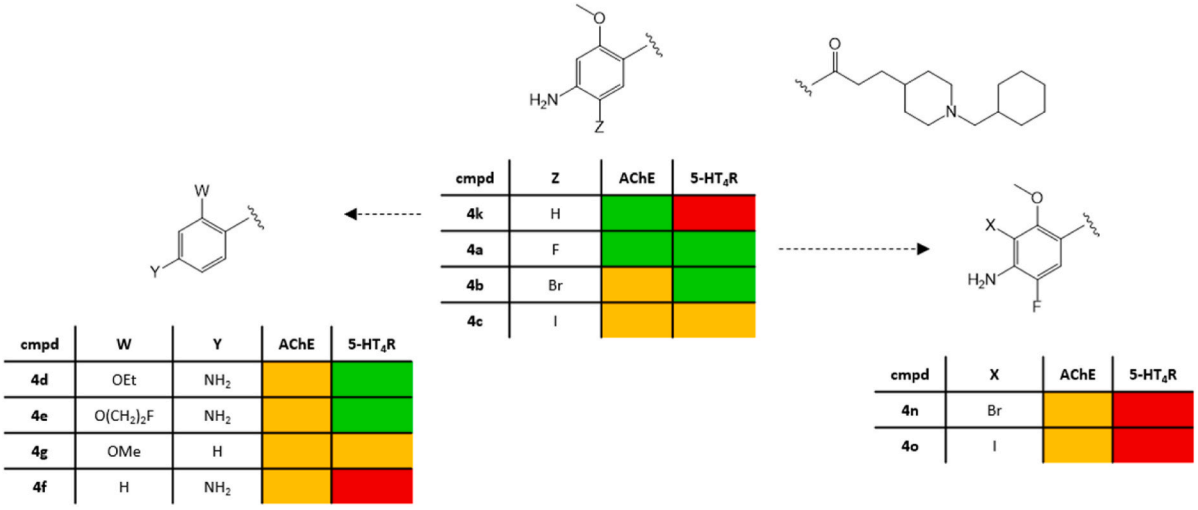


**Fig. 11.** Pharmacomodulations of donecopride: influence of the Z substituent (green: activity enhanced or maintained; orange: activity slightly decreased; red: activity lost).

activities in mice. These two activities, associated with an increased release *in vitro* of the neurotrophic protein sAPPα, account for a potential interest of flucopride towards AD. Further investigations in various animal models of the pathology are ongoing to establish a possible disease-modifying effect in AD of flucopride and, if any, to undertake its regulatory preclinical study.

## 5. Experimental section

### 5.1. Chemistry

All compounds are >95 % pure by HPLC analysis.

#### 5.1.1. General material and methods

All chemical reagents and solvents used in the synthesis were purchased from commercial sources without further purification. Melting points were determined on a STUART SMP50 melting apparatus. NMR spectra were recorded on a JEOL LAMBDA 400 NMR spectrometer (399.7 MHz for $^{1}$H and 100.4 MHz for $^{13}$C), on a Bruker AVANCE III 400 MHz Spectrometer (399.8 MHz for $^{1}$H, 100 MHz for $^{13}$C and 376.1 MHz for $^{19}$F), on a Bruker AVANCE III 500 MHz Spectrometer (500.1 MHz for $^{1}$H, 125.8 MHz for $^{13}$C and 476 MHz for $^{19}$F) or on a Bruker NEO 600 MHz spectrometer (600.2 MHz for $^{1}$H, 150.9 MHz for $^{13}$C and 564.6 Hz for $^{19}$F) in chloroform-*d*, methanol-*d4* or DMSO-$d_6$. Mass spectrometry was performed on a SQ detector by positive ESI. High resolution mass spectra were performed by electrospray on an Acquity UPLC H-Class-Xevo G2-XS QTof (Waters). Infrared spectra were obtained on a PERKINELMER FT-IR spectrometer and are reported in terms of frequency of absorption (*n*, cm-1) using KBr cells (solution of the product in DCM). Single crystals for X-ray crystallographic analysis were obtained by slow evaporation from a mixture of chloroform/acetone. Data for crystal structures analysis were collected at 150 K with a Bruker–Nonius Kappa CCD area detector diffractometer with graphite–monochromatized Mo $K_\lambda$ radiation ($\lambda = 0.71073$ Å). The structures were solved using direct methods and refined by full-matrix least-squares analysis on $F^2$. Crystallographic data have been deposited at the Cambridge Crystallographic Data Centre, CCDC. Copies of this information may be obtained free of charge from the Director, CCDC, 12 Union Road, Cambridge, CB2 1EZ, UK (+44-1223-336408; E-mail: deposit@ccdc.cam.ac.uk or http://www.ccdc.cam.ac.uk).

#### 5.1.2. 4-Amino-5-fluoro-2-methoxybenzoic acid (1a)

[15] To a stirred solution of MeOH (6.57 mL) in dry THF (35 mL) under $N_2$ was added *t*-BuOK (3.64 g, 32.44 mmol, 2.5 equiv) in 20 mL of dry THF at 0 °C in dropwise over 10 min. The resulting solution was stirred at room temperature for 15 min, and then 4-amino-2,

5-difluorobenzonitrile (2.0 g, 12.98 mmol) was added. The mixture was then stirred at 70 °C for 4.5 h. After evaporation of the solvent, the residue was diluted with EtOAc, washed with water and brine, dried over $MgSO_4$, and concentrated to dryness under reduced pressure. 4-amino-5-fluoro-2-methoxybenzonitrile was obtained and used without further purification (2.09 g, 94 % yield). $^1$H NMR ($CDCl_3$-*d*) $\delta$ 7.12 (d, $J = 10.3$ Hz, 1H), 6.26 (d, $J = 7.2$ Hz, 1H), 4.30 (br s, 2H), 3.83 (s, 3H). MS (ESI) $[M + H]^+ = 167.36$. A solution of 4-amino-5-fluoro-2--methoxybenzonitrile (1.7 g, 10.24 mmol) and KOH (8.74 g, 21.33 mmol, 2.1 equiv) in a mixture of 40 mL of EtOH/water (1/1) was heated at reflux for 24 h. The mixture was cooled and concentrated in *vacuo*. The residue was acidified until pH4 with HCl 3 N and then extracted twice with EtOAc. The crude product was then purified on silica gel (gradient of elution: DCM to DCM/EtOAc 8/2) to afford 1.31 g of product (70 % yield). mp 187–189 °C. $^1$H NMR ($CDCl_3$-*d*) $\delta$ 7.77 (d, $J = 11.7$ Hz, 1H), 6.34 (d, $J = 6.8$ Hz, 1H), 4.00 (s, 3H). $^{13}$C NMR ($CD_3OD$-$d_4$) $\delta$ 167.1, 157.7, 144.6 (d, $J = 230.6$ Hz), 143.0 (d, $J = 14.6$ Hz), 117.7 (d, $J = 20.1$ Hz), 104.7 (d, $J = 6.2$ Hz), 98.0 (d, $J = 6.2$ Hz), 55.4. $^{19}$F NMR ($CDCl_3$-*d*) = −144.50. MS (ESI) *m/z* $[M + H]^- = 183.96$.

### 5.1.3. 4-Amino-5-bromo-2-methoxybenzoic acid (1b)

To a mixture of 4-amino-2-methoxybenzoic acid (1 g, 5.98 mmol) and NBS (1.065 g, 5.98 mmol, 1.0 equiv.) was added dioxane (40 mL). The reaction mixture was stirred at room temperature for 1 h. Evaporation of the solvent provided white residue which was diluted in EtOAc, washed with water, then dried over $MgSO_4$ and purified by column on silica (cyclohexane/EtOAc, gradient of elution 80/20 to 40/60) to give **1b** (1.210 g, 82 % yield) as white crystals. mp 192–194 °C. $^1$H NMR ($CDCl_3$-*d*) $\delta$ 10.32 (br s, 1H), 8.23 (s, 1H), 6.33 (s, 1H), 4.66 (br s, 2H, $NH_2$), 4.01 (s, 3H). $^{13}$C NMR (DMSO-$d_6$) $\delta$ 165.3, 160.1, 150.9, 135.9, 97.7, 97.5, 97.0, 55.5. MS (ESI) *m/z* $[M + H]^+ = 246.04/247.90$. IR ($cm^{-1}$) $\nu$ 3459, 3344, 1635, 1590, 1208.

### 5.1.4. 4-Amino-5-iodo-2-methoxybenzoic acid [1c]

Similarly prepared with NIS, white crystals (65 % yield). mp 195–197 °C. $^1$H NMR ($CDCl_3$-*d*) $\delta$ 10.28 (br s, 1H), 8.43 (s, 1H), 6.30 (s, 1H), 4.67 (br s, 2H, $NH_2$), 4.01 (s, 3H). $^{13}$C NMR (DMSO-$d_6$) $\delta$ 165.2, 160.9, 153.5, 142.4, 109.5, 98.8, 70.7, 55.4. MS (ESI) *m/z* $[M + H]^+ = 294.03$. HRMS (ESI) *m/z* $[M+H]^+$ calcd for $C_{10}H_{14}NO_3$ 364.0046, found 364.0028. IR ($cm^{-1}$) $\nu$ 3459, 3332, 1699, 1582, 1207.

### 5.1.5. 4-Benzyloxybenzoic acid (1i)

To a stirred solution of 4-hydroxybenzoic acid (1.0 g, 7.24 mmol) in MeOH (35 mL) at 0 °C was added dropwise $SOCl_2$ (1.05 mL, 14.48 mmol, 2.0 equiv) and the resulting mixture was refluxed for 3h. After cooling to room temperature, the mixture was concentrated *in vacuo*. The residue was dissolved with EtOAc, and the organic layer was washed with a saturated $NaHCO_3$ solution and brine. The organic phase was dried over $MgSO_4$ and concentrated under reduced pressure to afford methyl 4-hydroxybenzoate as a pale yellow solid (1.01 g, 92 % yield). mp 125–127 °C. $^1$H NMR ($CDCl_3$-*d*) $\delta$ 7.95 (d, $J = 8.9$ Hz, 2H), 6.87 (d, $J = 8.8$ Hz, 2H), 3.89 (s, 3H). $^{13}$C NMR ($CDCl_3$-*d*) $\delta$ 167.7, 160.5, 132.2, 122.5, 115.5, 52.2. MS (ESI) *m/z* $[M - H]^-$ 151.32. IR ($cm^{-1}$) $\nu$ 3311, 2963, 2020, 1682, 1588, 1434, 1279, 1233, 1164. To a stirred solution of methyl 4-hydroxybenzoate (1.0 g, 6.57 mmol) in DMF (100 mL) was added $K_2CO_3$ (3.632 g, 26.28 mmol, 4.0 equiv) and the resulting mixture was cooled in an ice-water bath to allow at 0 °C the addition of benzyl bromide (858 μL, 7.23 mmol, 1.1 equiv). The resulting mixture was stirred overnight at room temperature, then concentrated *in vacuo* to remove DMF. The residue was dissolved with EtOAc and washed with brine. The organic layer was dried over $MgSO_4$ and concentrated *in vacuo*. The crude was purified by chromatography on silica gel column (cyclohexane/EtOAc, gradient of elution 100/0 to 80/20) to afford methyl 4-benzyloxybenzoate [15] as a pale yellow solid (931 mg, 58 % yield). mp 85–87 °C. $^1$H NMR ($CDCl_3$-*d*) $\delta$ 8.00 (d, $J = 8.8$ Hz, 2H), 7.45–7.32 (m, 5H), 6.99 (d, $J = 8.8$ Hz, 2H), 5.12 (s, 2H), 3.88 (s, 3H). $^{13}$C NMR ($CDCl_3$-*d*) $\delta$ 167.1, 162.7, 136.4, 131.8, 128.9, 128.4, 127.7, 123.0, 114.6, 70.2, 52.0. MS (ESI): *m/z* $[M+H]^+$ 243.48. IR ($cm^{-1}$) $\nu$ 3031, 2953, 2846, 1715, 1605, 1251, 1011. To a stirred solution of methyl 4-benzyloxybenzoate (1.16 g, 4.79 mmol) in EtOH (50 mL) was added a 1 N NaOH solution (48 mL, 10 equiv) under $N_2$ at room temperature. The resulting mixture was stirred overnight at room temperature, and concentrated *in vacuo* to remove EtOH. The residue was diluted with water. The aqueous layer was acidified by addition of hydrochloric acid until acidic pH, and extracted several times with EtOAc. The combined organic extract was washed with brine, dried over $MgSO_4$ and concentrated under reduced pressure to afford 4-benzyloxybenzoic acid [16] as a pale yellow solid (930 mg, 85 % yield). mp 187–189 °C. $^1$H NMR ($CDCl_3$-*d*) $\delta$ 8.06 (d, $J = 8.9$ Hz, 2H), 7.49–7.31 (m, 5H), 7.02 (d, $J = 8.9$ Hz, 2H), 5.14 (s, 2H). $^{13}$C NMR ($CDCl_3$-*d*) $\delta$ 171.5, 163.5, 136.4, 132.7, 129.0, 128.6, 127.8, 122.1, 114.9, 70.4. MS (ESI) *m/z* $[M+H]^+$ 229.59. IR ($cm^{-1}$) $\nu$ 3040-2545, 3038, 2925, 2872, 2665, 1685, 1607, 1257, 1169.

### 5.1.6. 4-Benzyloxy-5-chloro-2-methoxybenzoic acid (1j)

To a stirred solution of 4-amino-2-methoxybenzoic acid (2.0 g, 12.0 mmol, 1.0 equiv) in a mixture of $H_2SO_4$ conc./$H_2O$ (1/1–40 mL) was added by portion $NaNO_2$ (828 mg, 12.0 mmol, 1.0 equiv) at 0 °C under $N_2$. The resulting mixture was stirred for 30 min at 0 °C, then at room temperature for 48 h. The reaction was diluted with EtOAc, and washed with brine. The organic layer was dried over $MgSO_4$ and was concentrated *in vacuo*. The crude was purified by chromatography on silica gel column eluting with cyclohexane/EtOAc (40/60) to afford 4-hydroxy-2-methoxybenzoic acid as an orange solid (1.66 g, 82 % yield). mp 194–196 °C. $^1$H NMR (DMSO-$d_6$) $\delta$ 7.60 (d, $J = 8.4$ Hz, 1H), 6.44 (d, $J = 2.2$ Hz, 1H), 6.38 (dd, $J = 8.6$ Hz, $J = 2.2$ Hz, 1H), 3.75 (s, 3H). $^{13}$C NMR (DMSO-$d_6$) $\delta$ 166.7, 162.9, 161.1, 133.7, 110.9, 107.2, 99.6, 55.5. MS (ESI) *m/z* $[M+H]^+$ 169.36. IR ($cm^{-1}$) $\nu$ 3203, 2955, 2847, 1701, 1610, 1269. To a stirred solution of 4-hydroxy-2-methoxybenzoic acid (1.47 g, 8.74 mmol) in MeOH (40 mL) at 0 °C was added dropwise $SOCl_2$ (1.27 mL, 17.48 mmol, 2.0 equiv) and the resulting mixture was refluxed for 3h. After cooling to room temperature, the mixture was concentrated *in vacuo*. The residue was dissolved in EtOAc, and the organic layer was washed with a saturated $NaHCO_3$ solution and brine. The organic phase was dried over $MgSO_4$ and concentrated under reduced pressure to afford methyl 4-hydroxy-2-methoxybenzoate [17] as an orange solid (1.14 g, 72 % yield). mp 149–151 °C. $^1$H NMR ($CDCl_3$-*d*) $\delta$ 7.80 (d, $J = 8.5$ Hz, 1H), 6.46 (d, $J = 2.2$ Hz, 1H), 6.42 (dd, $J = 8.5$ Hz, $J = 2.2$ Hz, 1H), 5.54 (br s, 1H, OH), 3.87 (s, 3H), 3.85 (s, 3H). $^{13}$C NMR ($CDCl_3$-*d*) $\delta$ 166.4, 161.9, 160.9, 134.3, 112.3, 107.3, 99.7, 56.1, 51.9. MS (ESI) *m/z* $[M - H]^-$ 181.31. IR ($cm^{-1}$) $\nu$ 3299, 2950, 2839, 1700, 1579, 1254, 1195, 1100. To a stirred solution of methyl 4-hydroxy-2-methoxybenzoate (900 mg, 4.94 mmol, 1.0 equiv) in dioxane (30 mL) was added *N*-chlorosuccinimide (725 mg, 5.43 mmol, 1.1 equiv) and the resulting mixture was refluxed for 20 h. After cooling to room temperature, the mixture was concentrated *in vacuo*. The residue was dissolved with EtOAc, and washed with brine. The organic layer was dried over $MgSO_4$ and was concentrated *in vacuo*. The crude was purified by chromatography on silica gel column (DCM/EtOAc, gradient of elution 50/50 to 0/100) and concentrated under reduced pressure to afford methyl 5-chloro-4-hydroxy-2-methoxybenzoate as an orange solid (782 mg, 73 % yield). mp 190–192 °C. $^1$H NMR ($CDCl_3$-*d*) $\delta$ 7.89 (s, 1H), 6.64 (s, 1H), 5.89 (br s, 1H, OH), 3.88 (s, 3H), 3.86 (s, 3H). $^{13}$C NMR ($CDCl_3$-*d*) $\delta$ 165.1, 160.5, 155.9, 132.7, 113.1, 111.1, 100.3, 56.5, 52.2. MS (ESI) *m/z* $[M+H]^+$ 217.30/219.34. HRMS (ESI) *m/z* $[M+H]^+$ calcd for $C_9H_{10}ClO_4$ 217.0262, found 217.0263. IR ($cm^{-1}$) $\nu$ 3191, 2959, 1689, 1601, 1435, 1252, 1108. To a stirred solution of methyl 5-chloro-4-hydroxy-2-methoxy benzoate (80 mg, 0.37 mmol) in DMF (7 mL) was added $K_2CO_3$ (205 mg, 1.48 mmol, 4.0 equiv) and the resulting mixture was cooled in an ice-water bath to allow at 0 °C the addition of benzyl bromide (48 μL, 0.41 mmol, 1.1 equiv). The resulting mixture was stirred overnight at room temperature, then concentrated *in vacuo* to

remove DMF. The residue was dissolved in EtOAc and washed with brine. The organic layer was dried over $MgSO_4$ and concentrated *in vacuo*. The crude was purified by chromatography on silica gel column (cyclohexane/EtOAc, gradient of elution 100/0 to 80/20) to obtain methyl 4-benzyloxy-5-chloro-2-methoxy-benzoate as a pale yellow solid (86 mg, 76 % yield). mp 105–107 °C. $^1$H NMR ($CDCl_3$-*d*) $\delta$ 7.91 (s, 1H), 7.46–7.32 (m, 5H), 6.53 (s, 1H), 5.21 (s, 2H), 3.85 (s, 3H), 3.83 (s, 3H). $^{13}$C NMR ($CDCl_3$-*d*) $\delta$ 165.2, 160.1, 158.3, 135.8, 133.5, 128.9, 128.5, 127.2, 114.3, 112.7, 98.6, 71.0, 56.4, 52.0. MS (ESI) *m/z* $[M+H]^+$ 307.35/309.31. HRMS (ESI) *m/z* $[M+H]^+$ calcd for $C_{16}H_{16}ClO_4$ 307.0732, found 307.0729. IR ($cm^{-1}$) $\nu$ 3038, 2952, 1690, 1598, 1279, 1232, 1113, 1008. To a stirred solution of methyl 4-benzyloxy-5-chloro-2-methoxybenzoate (200 mg, 0.65 mmol) in EtOH (10 mL) was added a 1 N NaOH solution (6.54 mL, 6.54 mmol, 10.0 equiv) under $N_2$ at room temperature. The resulting mixture was stirred overnight at room temperature, and concentrated *in vacuo* to remove EtOH. The residue was diluted with water. The aqueous layer was acidified by addition of HCl until acidic pH, and extracted several times with EtOAc. The combined organic extract was washed with brine, dried over $MgSO_4$ and concentrated under reduced pressure to afford the expected benzoic acid (174 mg, 91 % yields) as a white solid. mp 171–173 °C. $^1$H NMR ($CDCl_3$-*d*) $\delta$ 10.30 (br s, 1H, OH), 8.20 (s, 1H), 7.47–7.35 (m, 5H), 6.58 (s, 1H), 5.26 (s, 2H), 4.00 (s, 3H). $^{13}$C NMR ($CDCl_3$-*d*) $\delta$ 164.2, 159.2, 158.1, 135.4, 134.9, 129.1, 128.8, 127.2, 121.9, 110.9, 97.9, 71.4, 57.1. MS (ESI) *m/z* $[M+H]^+$ 293.37/295.33. HRMS (ESI) *m/z* $[M+H]^+$ calcd for $C_{15}H_{14}ClO_4$ 293.0575, found 293.0573. IR ($cm^{-1}$) $\nu$ 3070-2524, 2941, 1675, 1599, 1271, 1245, 1005.

### 5.1.7. General procedure for the synthesis of β-keto ester

To a stirred solution of benzoic acid derivative (1.0 equiv) in dry THF (10 mL/mmol) was added CDI (1.1 equiv) and the resulting mixture was stirred at room temperature for 5–7 h. Then potassium 3-ethoxy-3-oxopropanoate (1.2 equiv) and $MgCl_2$ (1.2 equiv) were added portion-wise. The reaction mixture was stirred for 14–48 h, and was concentrated *in vacuo*. The residue was dissolved with EtOAc, then the organic layer was washed with a saturated $NaHCO_3$ solution and brine, and was dried over $MgSO_4$. Removal of the solvent under vacuum afforded the crude product, which was purified by chromatography on silica gel column and concentrated under reduced pressure to afford β-keto ester compound (22–80 % isolated yields).

### 5.1.8. Ethyl 3-(4-amino-5-fluoro-2-methoxyphenyl)-3-oxopropanoate [2a]

Pale yellow powder (73 % yield). mp 81–83 °C. $^1$H NMR ($CDCl_3$-*d*) $\delta$ 7.63 (d, 1H), 6.23 (d, 1H), 4.27 (br s, 2H), 4.17 (qd, $J$ = 7.1 Hz, 2H), 3.87 (s, 2H), 3.81 (s, 3H), 1.23 (t, $J$ = 7.2 Hz, 3H). $^{13}$C NMR ($CDCl_3$-*d*) $\delta$ 189.8, 168.7, 157.6, 145.6 ($J$ = 232.4 Hz), 141.2 ($J$ = 15.2 Hz), 117.1 ($J$ = 20.1 Hz), 115.6 ($J$ = 5.1 Hz), 98.0 ($J$ = 3.0 Hz), 60.8, 55.6, 50.5, 14.2. $^{19}$F NMR ($CDCl_3$-*d*) −145.69. MS (ESI) $[M+H]^+$ = 278.45. HRMS (ESI) *m/z* $[M+H]^+$ calcd for $C_{12}H_{15}FNO_4$ 256.0985, found 256.0987. IR ($cm^{-1}$) $\nu$ 3470, 3364, 3231, 2982, 1730, 1653, 1628, 1604, 1522, 1470, 1367, 1319.

### 5.1.9. Ethyl 3-(4-amino-5-bromo-2-methoxyphenyl)-3-oxopropanoate [2b]

White solid (50 % yield). mp 129–131 °C. $^1$H NMR ($CDCl_3$-*d*) $\delta$ 8.08 (s, 1H), 6.23 (s, 1H), 4.59 (s, 2H), 4.18 (q, $^3J$ = 7.8 Hz, 2H), 3.87 (s, 2H), 3.83 (s, 3H), 1.24 (t, $J$ = 7.8 Hz, 3H). $^{13}$C NMR ($CDCl_3$-*d*) $\delta$ 189.5, 168.6, 160.4, 149.8, 135.8, 117.8, 100.7, 96.8, 60.8, 55.3, 50.4, 14.1. MS (ESI) *m/z* $[M+H]^+$ = 316.05/318.04. IR ($cm^{-1}$) $\nu$ 3456, 3357, 2981, 1724, 1620, 1321, 1023. HRMS (ESI) *m/z* $[M+H]^+$ calcd for $C_{12}H_{15}BrNO_4$ 326.0184, found 326.0187.

### 5.1.10. Ethyl 3-(4-amino-5-iodo-2-methoxyphenyl)-3-oxopropanoate [2c]

White solid (55 % yield) mp 139–141 °C. $^1$H NMR ($CDCl_3$-*d*) $\delta$ 8.25 (s, 1H), 6.22 (s, 1H), 4.65 (br s, 2H, $NH_2$), 4.17 (q, $J$ = 7.8 Hz, 2H), 3.87 (s, 2H), 3.82 (s, 3H), 1.24 (t, $J$ = 7.8 Hz, 3H). $^{13}$C NMR ($CDCl_3$-*d*) $\delta$ 189.3, 168.6, 161.4, 152.3, 142.3, 118.6, 95.9, 73.5, 60.8, 55.3, 50.3, 14.2. IR ($cm^{-1}$) $\nu$ 3454, 3350, 2979, 1732, 1619, 1325, 1226, 1032. HRMS (ESI) *m/z* $[M+H]^+$ calcd for $C_{12}H_{15}INO_4$ 364.0046, found 364.0028. MS *m/z* $[M + H]^+$ = 364.07.

### 5.1.11. Ethyl 3-(4-amino-2-ethoxy-phenyl)-3-oxopropanoate (2d)

[18] White solid (23 % yield). mp 118–120 °C. $^1$H NMR ($CDCl_3$-*d*) $\delta$ 7.82 (d, $^3J$ = 8.6 Hz, 1H), 6.25 (dd, $J$ = 8.6 Hz, $J$ = 2.1 Hz, 1H), 6.10 (d, $J$ = 2.0 Hz, 1H), 4.18 (q, $J$ = 7.1 Hz, 2H), 4.05 (q, $J$ = 7.0 Hz, 2H), 3.94 (s, 2H), 1.45 (t, $J$ = 7.0 Hz, 3H), 1.24 (t, $J$ = 7.1 Hz, 3H). $^{13}$C NMR ($CDCl_3$-*d*) $\delta$ 190.9, 169.2, 161.3, 153.2, 133.7, 117.1, 107.4, 97.1, 64.1, 60.9, 50.7, 14.7, 14.3. MS (ESI) *m/z* $[M+H]^+$ 252.49. HRMS (ESI) *m/z* $[M+H]^+$ calcd for $C_{13}H_{18}NO_4$ 252.1230, found 252.1227. IR ($cm^{-1}$) $\nu$ 3477, 3381, 3244, 2977, 2938, 2889, 1720, 1594, 1457, 1338, 1204, 1017.

### 5.1.12. Ethyl 3-[4-amino-2-(2-fluoroethoxy)phenyl]-3-oxopropanoate [2e]

[19] White solid (36 % yield). mp 116–118 °C. $^1$H NMR ($CDCl_3$-*d*) $\delta$ 7.85 (d, $J$ = 8.6 Hz, 1H), 6.30 (dd, $J$ = 8.6 Hz, $J$ = 2.1 Hz, 1H), 6.09 (d, $J$ = 2.0 Hz, 1H), 4.79 (dt, $J$ = 47.3 Hz, $J$ = 4.1 Hz, 2H), 4.24 (dt, $J$ = 27.6 Hz, $J$ = 4.2 Hz, 2H), 4.18 (q, $J$ = 7.1 Hz, 2H), 3.96 (s, 2H), 1.24 (t, $J$ = 7.1 Hz, 3H). $^{13}$C NMR ($CDCl_3$-*d*) $\delta$ 190.8, 169.1, 160.5, 153.2, 133.8, 117.2, 108.1, 97.3, 81.5 (d, $J$ = 170.8 Hz), 67.6 (d, $J$ = 20.3 Hz), 61.0, 50.6, 14.2. $^{19}$F NMR ($CDCl_3$-*d*) $\delta$ −223.19. MS (ESI) *m/z* $[M+H]^+$ 270.45. HRMS (ESI) *m/z* $[M+H]^+$ calcd for $C_{13}H_{17}FNO_4$ 270.1136, found 270.1132. IR ($cm^{-1}$) $\nu$ 3471, 3375, 3244, 2990, 2962, 2927, 2854, 1710, 1612, 1446, 1341, 1208, 1015.

### 5.1.13. Ethyl 3-(4-aminophenyl)-3-oxopropanoate [2f]

Yellow oil (38 % yield). $^1$H NMR ($CDCl_3$-*d*) $\delta$ 7.79 (d, $J$ = 8.8 Hz, 2H), 6.64 (d, $J$ = 8.8 Hz, 2H), 4.20 (q, $J$ = 7.2 Hz, 2H), 3.89 (s, 2H), 1.25 (t, $J$ = 7.2 Hz, 3H). $^{13}$C NMR ($CDCl_3$-*d*) $\delta$ 190.6, 168.2, 151.8, 131.3, 126.7, 113.9, 61.5, 45.8, 14.3. MS (ESI) *m/z* $[M+H]^+$ 208.45. HRMS (ESI) *m/z* $[M+H]^+$ calcd for $C_{11}H_{14}NO_3$ 208.0968, found 208.0965. IR ($cm^{-1}$) $\nu$ 3476, 3371, 3239, 2982, 2939, 1732, 1595, 1222, 1036, 840, 567.

### 5.1.14. Ethyl 3-(2-methoxyphenyl)-3-oxopropanoate (2g)

Colorless oil (22 % yield). $^1$H NMR ($CDCl_3$-*d*) $\delta$ 7.88 (dd, $J$ = 7.8 Hz, $J$ = 1.8 Hz, 1H), 7.50 (ddd, $J$ = 8.5 Hz, $J$ = 7.4 Hz, $J$ = 1.8 Hz, 1H), 7.03 (m, 1H), 6.96 (d, $J$ = 8.4 Hz, 1H), 4.18 (q, $J$ = 7.2 Hz, 2H), 3.96 (s, 2H), 3.89 (s, 3H), 1.23 (t, $J$ = 7.2 Hz, 3H). $^{13}$C NMR ($CDCl_3$-*d*) $\delta$ 193.1, 168.2, 159.1, 134.7, 131.1, 126.3, 120.9, 111.5, 60.9, 55.3, 50.7, 14.1. MS (ESI) *m/z* $[M+H]^+$ 223.41.

### 5.1.15. Ethyl 3-(4-amino-3-chlorophenyl)-3-oxopropanoate (2h)

Pale yellow solid (65 % yield). mp 96–98 °C. $^1$H NMR ($CDCl_3$-*d*) $\delta$ 7.89 (d, $J$ = 1.9 Hz, 1H), 7.68 (dd, $J$ = 8.3 Hz, $J$ = 1.7 Hz, 1H), 6.74 (d, $J$ = 8.3 Hz, 1H), 4.65 (br s, 2H, $NH_2$), 4.20 (q, $J$ = 7.3 Hz, 2H), 3.87 (s, 2H), 1.25 (t, $J$ = 7.1 Hz, 3H). $^{13}$C NMR ($CDCl_3$-*d*) $\delta$ 189.8, 167.9, 148.0, 130.8, 129.2, 127.1, 118.6, 114.5, 61.6, 45.7, 14.2. MS (ESI) *m/z* $[M+H]^+$ 242.41/244.47. HRMS (ESI) *m/z* $[M+H]^+$ calcd for $C_{11}H_{13}ClNO_3$ 242.0578, found 242.0576. IR ($cm^{-1}$) $\nu$ 3452, 3355, 2995, 2981, 2952, 1704, 1586, 1336, 1205, 1020.

### 5.1.16. Ethyl 3-(4-benzyloxyphenyl)-3-oxopropanoate (2i)

Pale yellow solid (80 % yield). mp 62–64 °C. $^1$H NMR ($CDCl_3$-*d*) $\delta$ 7.93 (d, $J$ = 8.9 Hz, 2H), 7.44–7.33 (m, 5H), 7.02 (d, $J$ = 9.0 Hz, 2H), 5.14 (s, 2H), 4.21 (q, $J$ = 7.2 Hz, 2H), 3.94 (s, 2H), 1.25 (t, $J$ = 7.1 Hz, 3H). $^{13}$C NMR ($CDCl_3$-*d*) $\delta$ 191.3, 168.0, 163.4, 136.2, 131.1, 129.5, 128.9, 128.5, 127.7, 115.0, 70.3, 61.6, 45.9, 14.2. MS (ESI) *m/z* $[M+H]^+$ 299.48. IR ($cm^{-1}$) $\nu$ 3034, 2977, 2953, 1749, 1677, 1601, 1573, 1257.

*5.1.17. Ethyl 3-(4-benzyloxy-5-chloro-2-methoxyphenyl)-3-oxopropanoate (2j)*

Pale yellow solid (79 % yield). mp 73–75 °C. $^1$H NMR ($CDCl_3$-*d*) $\delta$ 8.00 (s, 1H), 7.47–7.36 (m, 5H), 6.49 (s, 1H), 5.23 (s, 2H), 4.17 (q, $J$ = 7.3 Hz, 2H), 3.88 (s, 2H), 3.82 (s, 3H), 1.22 (t, $J$ = 7.1 Hz, 3H). $^{13}$C NMR ($CDCl_3$-*d*) $\delta$ 190.4, 168.5, 159.7, 159.2, 135.7, 132.8, 129.0, 128.6, 127.2, 119.7, 116.0, 97.6, 71.2, 61.1, 55.8, 50.6, 14.2. MS (ESI) *m/z* $[M+Na]^+$ 385.37/387.37. HRMS (ESI) *m/z* $[M+H]^+$ calcd for $C_{19}H_{20}ClO_5$ 363.0994, found 363.0991. IR ($cm^{-1}$) $\nu$ 2990, 2943, 1748, 1670, 1597, 1404, 1276, 1004.

*5.1.18. Ethyl 3-(4-amino-2-methoxyphenyl)-3-oxopropanoate (2k)*

Colorless oil (35 % yield). $^1$H NMR ($CDCl_3$-*d*) $\delta$ 7.82 (d, $J$ = 8.6 Hz, 1H), 6.26 (dd, $J$ = 8.6 Hz, $J$ = 2.1 Hz, 1H), 6.12 (d, $J$ = 2.0 Hz, 1H), 4.18 (br s, 2H, $NH_2$), 4.17 (q, $J$ = 7.1 Hz, 2H), 3.88 (s, 2H), 3.82 (s, 3H), 1.23 (t, $J$ = 7.1 Hz, 3H). $^{13}$C NMR ($CDCl_3$-*d*) $\delta$ 190.6, 169.1, 161.9, 153.4, 133.6, 116.7, 107.5, 96.4, 60.9, 55.1, 50.7, 14.3. MS (ESI) *m/z* $[M+H]^+$ 238.42. HRMS (ESI) *m/z* $[M+H]^+$ calcd for $C_{12}H_{16}NO_4$ 238.1079, found 238.1079. IR ($cm^{-1}$) $\nu$ 3455, 3356, 2980, 1723, 1624, 1321, 1021.

*5.1.19. General procedure for the alkylation followed by saponification-decarboxylation reaction*

*5.1.19.1. Preparation of alkylated β-keto ester compounds.* To a stirred solution of β-keto ester compound (1.0 equiv) in DMF (10 mL/mmol) were added $K_2CO_3$ (2.0 equiv) and *tert*-butyl 4-(iodomethyl)piperidine-1-carboxylate (1.2 equiv). The resulting mixture was stirred at room temperature for 24–48 h, then concentrated *in vacuo*. The residue was dissolved with EtOAc, then the organic layer was washed with brine and was dried over $MgSO_4$. Removal of the solvent under vacuum afforded the crude product, as an oil, which was used for the next synthetic step without any purification.

*5.1.19.2. Saponification-decarboxylation reaction.* To a stirred solution of alkylated β-keto ester derivative (1.0 equiv) in a mixture of EtOH/$H_2O$ (5/2) (24 mL/mmol) was added KOH (4.5 equiv). The resulting mixture was refluxed for 2–4 h, then concentrated *in vacuo*. EtOAc was added, the organic layer was washed with brine and dried over $MgSO_4$. Removal of the solvent under vacuum afforded the crude product, which was purified by chromatography on silica gel column and concentrated under reduced pressure to afford expected compound (30–88 % isolated yields over 2 steps).

*5.1.20. tert-Butyl 4-(3-(4-amino-5-fluoro-2-methoxyphenyl)-3-oxopropyl) piperidine-1-carboxylate [3a]*

Pale yellow powder (80 % yield). mp 115–117 °C. $^1$H NMR ($CDCl_3$-*d*) $\delta$ 7.55 (d, $J$ = 12.1 Hz, 1H), 6.23 (d, $J$ = 7.0 Hz, 1H), 4.16 (br s, 2H), 4.07 (m, 2H), 3.84 (s, 3H), 2.92 (t, $J$ = 7.6 Hz, 2H), 2.67 (m, 2H), 1.67 (m, 2H), 1.60 (m, 2H), 1.45 (s, 9H), 1.43 (m, 1H), 1.10 (m, 2H). $^{13}$C NMR ($CDCl_3$-*d*) $\delta$ 198.8, 157.1, 154.9, 145.4 ($J$ = 232.0 Hz), 140.0 ($J$ = 14.8 Hz), 117.0 ($J$ = 20.6 Hz), 117.0 ($J$ = 4.1 Hz), 98.5 ($J$ = 3.3 Hz), 79.2, 55.8, 43.8, 40.6, 35.7, 32.1, 31.1, 28.4. $^{19}$F NMR ($CDCl_3$-*d*) $\delta$ −145.99. MS (ESI) *m/z* $[M + H]^+$ = 380.90. HRMS (ESI) *m/z* $[M+H]^+$ calcd for $C_{20}H_{30}FN_2O_4$ 403.2009, found 403.2011. IR ($cm^{-1}$) $\nu$ 3438, 3355, 2924, 2854, 1676, 1628, 1609, 1428, 1250, 1268.

*5.1.21. tert-Butyl 4-(3-(4-amino-5-bromo-2-methoxyphenyl)-3-oxopropyl) piperidine-1-carboxylate [3b]*

White solid (68 % yield). mp 146–148 °C. $^1$H NMR ($CDCl_3$-*d*) δ 7.94 (s, 1H), 6.29 (s, 1H), 4.64 (br s, 2H, $NH_2$), 4.08 (m, 2H), 3.84 (s, 3H), 2.90 (m, 2H), 2.67 (m, 2H), 1.67 (m, 2H), 1.59 (m, 2H), 1.45 (s, 9H), 1.43 (m, 1H), 1.10 (m, 2H). $^{13}$C NMR ($CDCl_3$-*d*) δ 198.6, 160.0, 154.8, 149.0, 135.3, 119.1, 100.2, 97.3, 79.1, 55.6, 44.2, 40.5, 35.7, 32.0, 31.1, 28.4. MS (ESI) *m/z* $[M + H - BOC]^+$ = 341.15/343.17. HRMS (ESI) *m/z* $[M+H]^+$ calcd for $C_{20}H_{30}BrN_2O_4$ 463.1208, found 463.1214. IR ($cm^{-1}$) $\nu$ 3468, 1668, 1624, 1418, 1165.

*5.1.22. tert-Butyl 4-(3-(4-amino-5-iodo-2-methoxyphenyl)-3-oxopropyl) piperidine-1-carboxylate [3c]*

White solid (65 % yield). mp 151–153 °C. $^1$H NMR ($CDCl_3$-*d*) $\delta$ 8.13 (s, 1H), 6.25 (s, 1H), 4.51 (br s, 2H, $NH_2$), 4.08 (m, 2H), 3.85 (s, 3H), 2.90 (m, 2H), 2.67 (m, 2H), 1.67 (m, 2H), 1.59 (m, 2H), 1.45 (s, 9H), 1.43 (m, 1H), 1.10 (m, 2H). $^{13}$C NMR ($CDCl_3$-*d*) $\delta$ 198.5, 161.0, 151.4, 141.9, 120.3, 96.4, 79.2, 73.5, 60.4, 55.4, 53.4, 40.5, 35.7, 32.4, 31.1, 28.5. MS *m/z* $[M + H - BOC]^+$ = 389.13. HRMS (ESI) *m/z* $[M+Na]^+$ calcd for $C_{20}H_{29}FN_2NaO_4$ 511.1077, found 511.1070. IR ($cm^{-1}$) $\nu$ 3459, 3341, 2850, 1673, 1621, 1579, 1415, 1365, 1298, 1217, 1165, 1041.

*5.1.23. tert-Butyl 4-[3-(4-amino-2-ethoxyphenyl)-3-oxopropyl]piperidine-1-carboxylate [3d]*

Yellow oil (74 % yield). $^1$H NMR ($CDCl_3$-*d*) $\delta$ 7.69 (d, $J$ = 8.5 Hz, 1H), 6.23 (dd, $J$ = 8.5 Hz, $J$ = 2.1 Hz, 1H), 6.12 (d, $J$ = 2.0 Hz, 1H), 4.05 (m + q, $J$ = 7.0 Hz, 4H), 2.96 (t, $J$ = 7.3 Hz, 2H), 2.66 (m, 2H), 1.67–1.58 (m, 4H), 1.45 (t, $J$ = 7.0 Hz, 3H), 1.44 (s, 9H), 1.41 (m, 1H), 1.10 (m, 2H). $^{13}$C NMR ($CDCl_3$-*d*) $\delta$ 200.1, 160.7, 155.0, 152.2, 133.2, 118.6, 107.2, 97.6, 79.3, 63.9, 44.1, 40.9, 36.0, 32.2, 31.3, 28.6, 15.0. MS (ESI) *m/z* $[M+H]^+$ 377.57. HRMS (ESI) *m/z* $[M+H]^+$ calcd for $C_{21}H_{33}N_2O_4$ 377.2435, found 377.2435. IR ($cm^{-1}$) $\nu$ 3445, 3356, 3239, 2979, 2931, 2858, 1675, 1646, 1594, 1277, 1037.

*5.1.24. tert-Butyl 4-[3-[4-amino-2-(2-fluoroethoxy)phenyl]-3-oxopropyl] piperidine-1-carboxylate [3e]*

Yellow oil (70 % yield). $^1$H NMR ($CDCl_3$-*d*) $\delta$ 7.66 (d, $J$ = 8.5 Hz, 1H), 6.23 (dd, $J$ = 8.5 Hz, $J$ = 1.9 Hz,1H), 6.08 (d, $J$ = 1.9 Hz), 4.72 (dt, $J$ = 47.5 Hz, $J$ = 5.3 Hz, 2H), 4.32 (br s, 2H, $NH_2$), 4.16 (dt, $J$ = 5.3 Hz, $J$ = 28.0 Hz, 2H), 4.02 (m, 2H), 2.95 (t, $J$ = 7.4 Hz, 2H), 2.63 (m, 2H), 1.65–1.55 (m, 4H), 1.41 (s, 9H), 1.37 (m, 1H), 1.05 (m, 2H). $^{13}$C NMR ($CDCl_3$-*d*) $\delta$ 199.9, 160.0, 154.9, 152.7, 133.1, 118.0, 107.6, 97.4, 81.6 (d, $J$ = 170.9 Hz), 79.4, 67.4 (d, $J$ = 19.7 Hz), 43.7, 40.8, 35.8, 32.0, 31.1, 28.4. $^{19}$F NMR ($CDCl_3$-*d*) $\delta$ −223.28. MS (ESI) *m/z* $[M+H]^+$ 395.63. HRMS (ESI) *m/z* $[M+H]^+$ calcd for $C_{21}H_{32}FN_2O_4$ 395.2341, found 395.2341. IR ($cm^{-1}$) $\nu$ 3450, 3355, 3239, 2926, 2858, 1677, 1641, 1595, 1277, 1062.

*5.1.25. tert-Butyl 4-[3-(4-aminophenyl)-3-oxopropyl]piperidine-1-carboxylate [3f]*

Yellow oil (50 % yield). $^1$H NMR (399.8 MHz, $CDCl_3$-*d*) $\delta$ 7.78 (d, $^3J$ = 8.6 Hz, 2H), 6.63 (d, $^3J$ = 8.5 Hz, 2H), 4.21 (br s, 2H, $NH_2$), 4.07 (m, 2H), 2.87 (t, $^3J$ = 7.6 Hz, 2H), 2.65 (m, 2H), 1.69–1.62 (m, 4H), 1.44 (m, 10H), 1.11 (m, 2H). $^{13}$C NMR (100 MHz $CDCl_3$-*d*) $\delta$ 198.5, 154.9, 151.0, 130.5, 127.5, 113.8, 79.2, 44.0, 35.7, 35.0, 32.1, 31.2, 28.5. MS (ESI) *m/z* $[M+H]^+$ 333.53. HRMS (ESI) *m/z* $[M+H]^+$ calcd for $C_{19}H_{29}N_2O_3$ 333.2173, found 333.2169. IR ($cm^{-1}$) $\nu$ 3437, 3355, 3235, 2975, 2925, 2851, 1672, 1596, 1428, 1280, 1172.

*5.1.26. tert-Butyl 4-[3-(2-methoxyphenyl)-3-oxopropyl]piperidine-1-carboxylate (3g)*

Colorless oil (30 % yield). $^1$H NMR ($CDCl_3$-*d*) $\delta$ 7.63 (dd, $J$ = 7.7 Hz, $J$ = 1.8 Hz, 1H), 7.43 (ddd, $J$ = 8.6 Hz, $J$ = 7.5 Hz, $J$ = 1.8 Hz, 1H), 7.00–6.93 (m, 2H), 4.05 (m, 2H), 3.88 (s, 3H), 2.96 (t, $J$ = 7.6 Hz, 3H), 2.65 (m, 2H), 1.67–1.59 (m, 4H), 1.43 (m, 10H), 1.09 (m, 2H). $^{13}$C NMR ($CDCl_3$-*d*) $\delta$ 202.9, 158.4, 154.9, 133.4, 130.3, 128.6, 120.7, 111.6, 79.3, 55.6, 44.1, 40.9, 35.8, 32.1, 30.9, 28.5. MS (ESI) *m/z* $[M+Na]^+$ 370.49. HRMS (ESI) *m/z* $[M+H]^+$ calcd for $C_{20}H_{30}NO_4$ 348.2169, found 348.2169. IR ($cm^{-1}$) $\nu$ 2976, 2929, 2849, 1691, 1423, 1363, 1245, 1162.

*5.1.27. tert-Butyl 4-[3-(4-amino-3-chlorophenyl)-3-oxopropyl]piperidine-1-carboxylate (3h)*

Pale yellow solid (59 % yield). mp 128–130 °C. $^1$H NMR ($CDCl_3$-*d*) $\delta$ 7.88 (d, $J$ = 2.0 Hz, 1H), 7.69 (dd, $J$ = 8.6 Hz, $J$ = 2.0 Hz, 1H), 6.74 (d, $J$ = 8.5 Hz, 1H), 4.58 (br s, 2H, $NH_2$), 4.09 (m, 2H), 2.87 (t, $J$ = 7.6 Hz,

2H), 2.66 (m, 2H), 1.69–1.62 (m, 4H), 1.44 (m, 10H), 1.11 (m, 2H). $^{13}$C NMR ($CDCl_3$-*d*) $\delta$ 197.6, 155.0, 147.4, 130.2, 128.5, 128.1, 118.5, 114.5, 79.4, 44.2, 35.7, 35.1, 32.1, 31.0, 28.6. MS (ESI) *m/z* $[M+H]^+$ 367.54/369.55. HRMS (ESI) *m/z* $[M+H]^+$ calcd for $C_{19}H_{28}ClN_2O_3$ 367.1783, found 367.1781. IR ($cm^{-1}$) $\nu$ 3458, 3340, 2978, 2934, 2854, 1685, 1631, 1591, 1428, 1216, 1151.

### 5.1.28. *tert-Butyl 4-[3-(4-benzyloxyphenyl)-3-oxopropyl]piperidine-1-carboxylate (3i)*

Colorless oil (88 % yield). $^1$H NMR ($CDCl_3$-*d*) $\delta$ 7.93 (d, $J$ = 8.9 Hz, 2H), 7.45–7.33 (m, 5H), 7.01 (d, $J$ = 8.9 Hz, 2H), 5.13 (s, 2H), 4.08 (m, 2H), 2.94 (m, 2H), 2.67 (m, 2H), 1.71–1.60 (m, 4H), 1.45 (m, 10H), 1.10 (m, 2H). $^{13}$C NMR ($CDCl_3$-*d*) $\delta$ 199.1, 162.8, 155.1, 136.4, 130.5, 130.4, 128.9, 128.5, 127.7, 114.8, 79.4, 70.3, 44.3, 35.7, 35.4, 32.1, 31.0, 26.3. MS (ESI) *m/z* $[M+Na]^+$ 446.61. HRMS (ESI) *m/z* $[M+Na]^+$ calcd for $C_{26}H_{33}NNaO_4$ 446.2307, found 446.2313.

### 5.1.29. *tert-Butyl 4-[3-(4-benzyloxy-5-chloro-2-methoxyphenyl)-3-oxopropyl]piperidine-1- carboxylate (3j)*

Yellow oil (77 % yield). $^1$H NMR ($CDCl_3$-*d*) $\delta$ 7.84 (s, 1H), 7.46 (m, 2H), 7.41 (m, 2H), 7.35 (m, 1H), 6.51 (s, 1H), 5.23 (s, 2H), 4.06 (m, 2H), 3.84 (s, 3H), 2.92 (m, 2H), 2.66 (m, 2H), 1.67–1.58 (m, 4H), 1.46 (m, 10H), 1.09 (m, 2H). $^{13}$C NMR ($CDCl_3$-*d*) $\delta$ 199.6, 159.2, 158.2, 155.1, 135.9, 132.4, 129.0, 128.5, 127.2, 121.4, 115.5, 98.0, 79.4, 71.1, 56.0, 44.0, 40.8, 35.8, 32.2, 31.0, 28.5. MS (ESI) *m/z* $[M+H]^+$ 488.51/490.55. HRMS (ESI) *m/z* $[M+H]^+$ calcd for $C_{27}H_{35}ClNO_5$ 488.2198, found 488.2194. IR ($cm^{-1}$) $\nu$ 2971, 2927, 2857, 1689, 1594, 1404, 1275, 1166, 1015.

### 5.1.30. *tert-Butyl 4-(3-(4-amino-2-methoxyphenyl)-3-oxopropyl) piperidine-1-carboxylate (3k)*

Pale yellow oil (67 % yield). $^1$H NMR ($CDCl_3$-*d*) $\delta$ 7.70 (d, $J$ = 8.5 Hz, 1H), 6.25 (dd, $J$ = 8.5 Hz, $J$ = 2.1 Hz, 1H), 7.70 (d, $J$ = 2.1 Hz, 1H), 4.07 (m, 4H), 3.85 (s, 3H), 2.92 (m, 2H), 2.66 (m, 2H), 1.69–1.58 (m, 5H), 1.46 (m, 9H), 1.09 (m, 2H). $^{13}$C NMR (MHz, $CDCl_3$-*d*) $\delta$ 199.8, 161.3, 154.9, 152.2, 133.2, 118.3, 107.1, 96.9, 79.2, 55.3, 44.0, 40.0, 35.8, 32.1, 31.3, 28.5. MS (ESI) *m/z* $[M+H]^+$ 362.98. HRMS (ESI) *m/z* $[M+H]^+$ calcd for $C_{27}H_{35}ClNO_5$ 488.2198, found 488.2194. IR ($cm^{-1}$) $\nu$ 2974, 2931, 2851, 1676, 1642, 1596, 1468, 1431, 1278, 1163.

### 5.1.31. *General procedure for the synthesis of compounds 4a-w*

To a stirred solution of *tert*-butyl piperidine-1-carboxylate derivative (1.0 equiv) in DCM (20 mL/mmol) was added TFA (2 mL/mmol). The resulting mixture was stirred at room temperature for 1h. Removal of the solvent under vacuum afforded the crude product, which was directly engaged in the next step. The residue obtained (1.0 equiv) was dissolved in DMF (10 mL/mmol) and cyclohexylmethyl bromide (1.3 equiv) and $K_2CO_3$ (10.0 equiv) were added. The resulting mixture was stirred at 110 °C for 4 h, then concentrated *in vacuo*. EtOAc was added, the organic layer was washed several times with brine, dried over $MgSO_4$ and concentrated *in vacuo*. The crude was purified by chromatography on silica gel column and concentrated under reduced pressure to afford alkylated compound (19–79 % isolated yields).

### 5.1.32. *1-(4-Amino-5-fluoro-2-methoxyphenyl)-3-[1-(cyclohexylmethyl)-4-piperidyl] propan -1-one [4a]*

Pale yellow powder (42 % yield). mp 167−169 °C. $^1$H NMR ($CDCl_3$-*d*) $\delta$ 7.54 (d, $J$ = 12.1 Hz, 1H), 6.26 (d, $J$ = 7.1 Hz, 1H), 4.14 (br s, 2H), 3.84 (s, 3H), 2.91 (t, $J$ = 7.7 Hz, 2H), 2.84 (d, $J$ = 10.7 Hz, 2H), 2.06 (d, $J$ = 7.1 Hz, 2H), 1.83–1.55 (m, 12H), 1.47 (m, 1H), 1.28–1.15 (m, 5H), 0.85 (m, 2H). $^{13}$C NMR ($CDCl_3$-*d*) $\delta$ 199.3, 157.0, 145.5 (d, $J$ = 232.2 Hz), 139.9 (d, $J$ = 14.8 Hz), 117.2 (d, $J$ = 4.5 Hz), 117.0 (d, $J$ = 20.6 Hz), 98.5, 66.3, 55.8, 54.5, 41.0, 35.7, 35.2, 32.2, 32.1, 31.4, 26.8, 26.2. MS (ESI) *m/z* $[M + H]^+$ = 377.63. HRMS (ESI) *m/z* $[M+H]^+$ calcd for $C_{22}H_{34}FN_2O_2$ 377.2604, found 377.2598. IR ($cm^{-1}$) $\nu$ 3352, 3221, 2921, 2849, 1627, 1602, 1521, 1467, 1428, 1251.

### 5.1.33. *1-(4-Amino-5-bromo-2-methoxyphenyl)-3-[1-(cyclohexylmethyl)-4-piperidyl] propan-1-one [4b]*

Light yellow solid (65 % yield). mp 147–149 °C. $^1$H NMR ($CDCl_3$-*d*) $\delta$ 7.93 (s, 1H), 6.26 (s, 1H), 4.51 (br s, 2H, $NH_2$), 3.84 (s, 3H), 2.90–2.88 (m, 2H), 2.87–2.84 (m, 2H), 2.08 (d, $J$ = 5.6 Hz, 2H), 1.83–1.79 (m, 2H), 1.67–1.42 (m, 8H), 1.25–1.11 (m, 8H), 0.91–0.84 (m, 2H). $^{13}$C NMR ($CDCl_3$-*d*) $\delta$ 199.1, 160.1, 149.0, 135.3, 119.4, 100.2, 97.5, 66.2, 55.6, 54.5, 40.9, 35.7, 35.2, 32.1, 32.1, 31.3, 26.7, 26.1. MS (ESI) *m/z* $[M + H]^+$ = 440.27/438.26. HRMS (ESI) *m/z* $[M+H]^+$ calcd for $C_{22}H_{34}BrN_2O_2$ 436.1725, found 436.1722. IR ($cm^{-1}$) $\nu$ 3468, 3357, 2930, 1638, 1573, 1451, 1262.

### 5.1.34. *1-(4-Amino-5-iodo-2-methoxyphenyl)-3-[1-(cyclohexylmethyl)-4-piperidyl]propan-1-one [4c]*

Yellow solid (47 % yield). mp 167–169 °C. $^1$H NMR ($CDCl_3$-*d*) $\delta$ 8.11 (s, 1H), 6.24 (s, 1H), 4.47 (br s, 2H, $NH_2$), 3.84 (s, 3H), 2.88 (m, 2H), 2.83 (m, 2H), 2.07 (d, $J$ = 6.9 Hz, 2H), 1.81–1.57 (m, 11H), 1.47 (m, 1H), 1.27–1.12 (m, 6H), 0.90–0.81 (m, 2H). $^{13}$C NMR ($CDCl_3$-*d*) $\delta$ 199.0, 161.0, 151.3, 141.9, 120.4, 96.5, 73.2, 66.3, 55.4, 54.6, 40.8, 35.8, 35.2, 32.3, 32.1, 31.4, 26.8, 26.2. MS (ESI) *m/z* $[M + H]^+$ = 485.37. HRMS (ESI) *m/z* $[M+H]^+$ calcd for $C_{22}H_{34}IN_2O_2$ 485.1665, found 485.1659. IR ($cm^{-1}$) $\nu$ 3457, 3323, 2920, 1625, 1575, 1447, 1263, 1215.

### 5.1.35. *1-(4-Amino-2-ethoxyphenyl)-3-[1-(cyclohexylmethyl)-4-piperidyl] propan-1-one [4d]*

[18] Yellow solid (58 % yield). mp 83–85 °C. $^1$H NMR (399.8 MHz, $CDCl_3$-*d*) $\delta$ 7.68 (d, $^3J$ = 8.5 Hz, 1H), 6.23 (dd, $^3J$ = 8.5 Hz, $^4J$ = 2.1 Hz, 1H), 6.12 (d, $^4J$ = 2.0 Hz, 1H), 4.09 (br s, 2H, $NH_2$), 4.05 (q, $^3J$ = 7.0 Hz, 2H), 3.02 (m, 2H), 2.95 (t, $^3J$ = 7.4 Hz, 2H), 2.28 (m, 2H), 2.07 (m, 2H), 1.79–1.59 (m, 9H), 1.56 (m, 1H), 1.45 (t, $^3J$ = 7.0 Hz, 3H), 1.38 (m, 1H), 1.27–1.08 (m, 5H), 0.90 (m, 2H). $^{13}$C NMR (100 MHz, $CDCl_3$-*d*) $\delta$ 200.1, 160.8, 152.2, 133.2, 118.5, 107.1, 97.6, 65.4, 63.9, 54.2, 41.0, 35.2, 34.7, 32.1, 31.2, 31.0, 26.6, 26.1, 15.0. MS (ESI) *m/z* $[M+H]^+$ 373.63. HRMS (ESI) *m/z* $[M+H]^+$ calcd $C_{23}H_{37}N_2O_2$ 373.2850, found 373.2850. IR ($cm^{-1}$) $\nu$ 3445, 3349, 3242, 2919, 2846, 1637, 1587, 1454, 1273, 1036.

### 5.1.36. *1-[4-Amino-2-(2-fluoroethoxy)phenyl]-3-[1-(cyclohexylmethyl)-4-piperidyl]propan-1-one [4e]*

[18] Yellow solid (43 % yield). mp 71–73 °C. $^1$H NMR ($CDCl_3$-*d*) $\delta$ 7.70 (d, $J$ = 8.5 Hz, 1H), 6.27 (dd, $J$ = 8.5 Hz, $J$ = 2.0 Hz, 1H), 6.10 (d, $J$ = 2.0 Hz, 1H), 4.77 (dt, $J$ = 47.4 Hz, $J$ = 4.1 Hz, 2H), 4.22 (dt, $J$ = 4.1 Hz, $J$ = 27.6 Hz, 2H), 4.10 (br s, 2H, $NH_2$), 2.96 (t, $J$ = 7.6 Hz, 2H), 2.83 (m, 2H), 2.06 (d, $J$ = 7.0 Hz, 2H), 1.82–1.57 (m, 11H), 1.46 (m, 1H), 1.27–1.08 (m, 6H), 0.84 (m, 2H). $^{13}$C NMR ($CDCl_3$-*d*) $\delta$ 200.3, 160.0, 152.1, 133.3, 118.9, 107.8, 97.8, 81.7 (d, $J$ = 171.2 Hz), 67.5 (d, $J$ = 20.2 Hz), 66.4, 54.7, 41.3, 36.0, 35.4, 32.5, 32.3, 31.4, 26.9, 26.4. $^{19}$F NMR ($CDCl_3$-*d*) $\delta$ −223.3 (tt, $J$ = 47.1 Hz, $J$ = 27.8 Hz). MS (ESI) *m/z* $[M+H]^+$ 391.64. HRMS (ESI) *m/z* $[M+H]^+$ calcd for $C_{23}H_{36}FN_2O_2$ 391.2755, found 391.2755. IR ($cm^{-1}$) $\nu$ 3429, 3347, 3240, 2921, 2849-2768, 1637, 1591, 1443, 1274, 1069.

### 5.1.37. *1-(4-Aminophenyl)-3-[1-(cyclohexylmethyl)-4-piperidyl]propan-1-one [4f]*

Pale yellow solid (48 % yield). mp 89–91 °C.$^1$H NMR ($CDCl_3$-*d*) $\delta$ 7.80 (d, $J$ = 8.6 Hz, 2H), 6.64 (d, $J$ = 8.6 Hz, 2H), 4.12 (br s, 2H, $NH_2$), 2.89–2.82 (m, 4H), 2.07 (d, $J$ = 7.0 Hz, 2H), 1.83–1.62 (m, 11H), 1.46 (m, 1H), 1.30–1.12 (m, 6H), 0.85 (m, 2H). $^{13}$C NMR ($CDCl_3$-*d*) $\delta$ 199.0, 151.0, 130.6, 127.7, 113.9, 66.4, 54.6, 35.8, 35.5, 35.4, 32.4, 32.2, 31.6, 26.9, 26.3. MS (ESI) *m/z* $[M+H]^+$ 329.86. HRMS (ESI) *m/z* $[M+H]^+$ calcd for $C_{21}H_{33}N_2O$ 329.2587, found 329.2587. IR ($cm^{-1}$) $\nu$ 3460, 3351, 3232, 2920, 2849, 1654, 1589, 1449, 1177.

### 5.1.38. *3-[1-(Cyclohexylmethyl)-4-piperidyl]-1-(2-methoxyphenyl) propan-1-one (4g)*

Yellow oil (48 % yield). $^1$H NMR ($CDCl_3$-*d*) $\delta$ 7.66 (dd, $J$ = 7.7 Hz, $J$

= 1.8 Hz, 1H), 7.47 (ddd, $J$ = 8.4 Hz, $J$ = 7.4 Hz, $J$ = 1.8 Hz, 1H), 7.02 (m, 1H), 6.98 (d, $J$ = 8.3 Hz, 1H), 3.92 (s, 3H), 2.99 (t, $J$ = 7.6 Hz, 2H), 2.87 (m, 2H), 2.10 (d, $J$ = 7.0 Hz, 2H), 1.87–1.61 (m, 11H), 1.50 (m, 1H), 1.29–1.15 (m, 6H), 0.88 (m, 2H). $^{13}$C NMR ($CDCl_3$-*d*) $\delta$ 203.5, 158.4, 133.3, 130.3, 128.8, 120.8, 111.6, 66.4, 55.6, 54.7, 41.3, 35.8, 35.4, 32.4, 32.3, 31.2, 26.9, 26.4. MS (ESI) *m/z* $[M+H]^+$ 344.82. HRMS (ESI) *m/z* $[M+H]^+$ calcd for $C_{22}H_{34}NO_2$ 344.2584, found 344.2581. IR ($cm^{-1}$) $\nu$ 2922, 2850, 1672, 1597, 1485, 1285, 1245, 1024.

### 5.1.39. 1-(4-Amino-3-chlorophenyl)-3-[1-(cyclohexylmethyl)-4-piperidyl] propan-1-one (4h)

Pale yellow solid (71 % yield). mp 110–112 °C. $^1$H NMR ($CDCl_3$-*d*) $\delta$ 7.89 (d, $J$ = 2.0 Hz, 1H), 7.70 (dd, $J$ = 8.5 Hz, $J$ = 2.0 Hz, 1H), 6.74 (d, $J$ = 8.5 Hz, 1H), 4.50 (br s, 2H, $NH_2$), 2.86 (t, $J$ = 7.7 Hz, 2H), 2.83 (m, 2H), 2.07 (d, $J$ = 7.0 Hz, 2H), 1.81 (m, 2H), 1.75 (m, 2H), 1.73–1.64 (m, 7H), 1.47 (m, 1H), 1.28–1.11 (m, 6H), 0.85 (m, 2H). $^{13}$C NMR ($CDCl_3$-*d*) $\delta$ 198.1, 147.2, 130.3, 128.6, 128.4, 118.6, 114.6, 66.4, 54.6, 35.8, 35.5, 35.4, 32.4, 32.3, 31.3, 27.0, 26.4. MS (ESI) *m/z* $[M+H]^+$ 363.60/365.57. HRMS (ESI) *m/z* $[M+H]^+$ calcd for $C_{21}H_{32}ClN_2O$ 363.2198, found 363.2196. IR ($cm^{-1}$) $\nu$ 3413, 3329, 3219, 2919, 2849, 2804, 2765, 1666, 1640, 1588, 1219, 1196. Crystal system monoclinic, space group P $2_1$/n, $a$ = 9.1422(3) Å, $b$ = 8.5309(3) Å, $c$ = 25.0743(8) Å, β = 96.966(1)°, V = 1941.14(11) Å$^3$, Z = 4, calculated density = 1.242 g/cm$^3$, μ = 0.21 mm$^{-1}$, $R_{int}$ = 0.041, R[$F^2 > 2\sigma(F^2)$] = 0.045, w$R(F^2)$ = 0.109, S = 1.04.

### 5.1.40. 1-(4-Benzyloxyphenyl)-3-[1-(cyclohexylmethyl)-4-piperidyl] propan-1-one (4i)

White solid (47 % yield). mp 116–118 °C. $^1$H NMR ($CDCl_3$-*d*) $\delta$ 7.93 (d, $^3J$ = 7.5 Hz, 2H), 7.38 (m, 5H), 7.00 (d, $^3J$ = 7.5 Hz, 2H), 5.13 (s, 2H), 2.91 (m, 4H), 2.12 (d, $^3J$ = 6.5 Hz, 2H), 1.87 (m, 2H), 1.76 (m, 2H), 1.70 (m, 7H), 1.50 (m, 1H), 1.33 (m, 3H), 1.18 (m, 3H), 0.87 (m, 2H). $^{13}$C NMR ($CDCl_3$-*d*) $\delta$ 199.3, 162.6, 136.3, 130.5, 130.4, 128.8, 128.4, 127.6, 114.7, 70.3, 66.2, 54.5, 35.7, 35.6, 35.2, 32.2, 32.1, 31.2, 26.9, 26.3. MS (ESI) *m/z* $[M+H]^+$ 420.71. HRMS (ESI) *m/z* $[M+H]^+$ calcd for $C_{28}H_{38}NO_2$ 420.2897, found 420.2892. IR ($cm^{-1}$) $\nu$ 3033, 2922, 2847, 2798, 1668, 1599, 1262, 1171.

### 5.1.41. 1-(4-Benzyloxy-5-chloro-2-methoxyphenyl)-3-[1-(cyclohexylmethyl)-4-piperidyl] propan- 1-one (4j)

White solid (42 % yield). mp 117–119 °C. $^1$H NMR ($CDCl_3$-*d*) $\delta$ 7.83 (s, 1H), 7.46 (m, 2H), 7.41 (m, 2H), 7.35 (m, 1H), 6.50 (s, 1H), 5.22 (s, 2H), 3.83 (s, 3H), 2.87 (m, 4H), 2.10 (m, 2H), 1.84 (m, 2H), 1.75 (m, 2H), 1.71–1.64 (m, 5H), 1.58 (m, 2H), 1.49 (m, 1H), 1.26 (m, 3H), 1.23–1.13 (m, 3H), 0.87 (m, 2H). $^{13}$C NMR ($CDCl_3$-*d*) $\delta$ 199.9, 159.1, 158.1, 135.9, 132.3, 128.9, 128.5, 127.2, 121.5, 115.4, 98.0, 71.2, 66.3, 56.0, 54.6, 41.2, 35.7, 35.3, 32.3, 32.3, 31.2, 26.9, 26.3. MS (ESI) *m/z* $[M+H]^+$ 484.51/486.48. HRMS (ESI) *m/z* $[M+H]^+$ calcd for $C_{29}H_{39}ClNO_3$ 484.2613, found 484.2611. IR ($cm^{-1}$) $\nu$ 3027, 2924, 2849, 1662, 1593, 1402, 1276, 1024.

### 5.1.42. 3-[1-(Cyclohexylmethyl)-4-piperidyl]-1-(2-methoxyphenyl) propan-1-one (4k)

Yellow oil (48 % yield). $^1$H NMR ($CDCl_3$-*d*) $\delta$ 7.66 (dd, $J$ = 7.7 Hz, $J$ = 1.8 Hz, 1H), 7.47 (ddd, $J$ = 8.4 Hz, $J$ = 7.4 Hz, $J$ = 1.8 Hz, 1H), 7.02 (m, 1H), 6.98 (d, $J$ = 8.3 Hz, 1H), 3.92 (s, 3H), 2.99 (t, $J$ = 7.6 Hz, 2H), 2.87 (m, 2H), 2.10 (d, $J$ = 7.0 Hz, 2H), 1.87–1.61 (m, 11H), 1.50 (m, 1H), 1.29–1.15 (m, 6H), 0.88 (m, 2H). $^{13}$C NMR ($CDCl_3$-*d*) $\delta$ 203.5, 158.4, 133.3, 130.3, 128.8, 120.8, 111.6, 66.4, 55.6, 54.7, 41.3, 35.8, 35.4, 32.4, 32.3, 31.2, 26.9, 26.4. MS (ESI) *m/z* $[M+H]^+$ 344.82. HRMS (ESI) *m/z* $[M+H]^+$ calcd for $C_{22}H_{34}NO_2$ 344.2584, found 344.2581. IR ($cm^{-1}$) $\nu$ 2922, 2850, 1672, 1597, 1485, 1285, 1245, 1024.

### 5.1.43. 3-[1-(Cyclohexylmethyl)-4-piperidyl]-1-(4-hydroxyphenyl) propan-1-one (4l)

To a stirred solution of **4i** (80 mg, 0.19 mmol, 1.0 equiv) in MeOH (25 mL) was charged Pd/C (20 mg, 10 mol%) and the mixture was stirred for 48h under $H_2$ at room temperature. The solution was filtered through a pad of Celite and evaporated. The crude was purified by flash chromatography on silica gel column (DCM/MeOH, gradient of elution 100/0 to 95/5) and concentrated under reduced pressure to afford the compound **(4l)**, as a pale yellow solid (22 mg, 35 % isolated yield). mp 93–95 °C. $^1$H NMR (MeOD-$d_4$) $\delta$ 7.87 (d, $J$ = 8.8 Hz, 2H), 6.81 (d, $J$ = 8.8 Hz, 2H), 3.01 (m, 2H), 2.95 (t, $J$ = 7.6 Hz, 2H), 2.28 (d, $J$ = 8.8 Hz, 2H), 2.09 (m, 2H), 1.79–1.60 (m, 9H), 1.58 (m, 1H), 1.44–1.14 (m, 6H), 0.93 (m, 2H). $^{13}$C NMR (MeOD-$d_4$) $\delta$ 201.4, 164.9, 131.9, 129.3, 116.6, 66.8, 55.3, 55.3, 36.2, 35.9, 33.0, 32.3, 32.2, 27.6, 27.1. MS (ESI) *m/z* $[M+H]^+$ 330.62. HRMS (ESI) *m/z* $[M+H]^+$ calcd for $C_{21}H_{32}NO_2$ 330.2433, found 330.2434. IR ($cm^{-1}$) $\nu$ 3431, 2922, 2851, 1676, 1605, 1445, 1264.

### 5.1.44. 1-(5-Chloro-4-hydroxy-2-methoxyphenyl)-3-[1-(cyclohexylmethyl)-4-piperidyl] propan-1-one (4 m)

To the compound **(4j)** (100 mg, 0.21 mmol, 1.0 equiv) was added a hydrobromic acid solution (33 wt% in acetic acid, 15 mL). The resulting mixture was stirred at room temperature for 4 h, and was poured slowly into a mixture water/ice. The residue was then extracted with EtOAc. The organic layer was washed several times with brine, dried over $MgSO_4$ and concentrated *in vacuo*. The crude was purified by flash chromatography on silica gel column (DCM/MeOH, gradient of elution 100/0 to 95/5) and concentrated under reduced pressure to afford the compound **(4m)**, as a white solid (31 mg, 37 % isolated yield). mp 92–94 °C. $^1$H NMR ($CDCl_3$-*d*) $\delta$ 7.80 (s, 1H), 6.52 (s, 1H), 5.87 (br s, 1H, OH), 3.74 (s, 3H), 3.27 (m, 2H), 2.85 (t, $J$ = 7.5 Hz, 2H), 2.50 (d, $J$ = 6.5 Hz, 2H), 2.30 (m, 2H), 1.83 (m, 2H), 1.77–1.53 (m, 10H), 1.43 (m, 1H), 1.26–1.09 (m, 3H), 0.96 (m, 2H). $^{13}$C NMR ($CDCl_3$-*d*) $\delta$ 199.0, 160.1, 160.0, 131.9, 119.2, 114.1, 100.8, 64.8, 55.8, 53.9, 40.6, 34.5, 34.1, 32.1, 30.8, 30.0, 26.2, 26.0. MS (ESI) *m/z* $[M+H]^+$ 394.50/396.46. HRMS (ESI) *m/z* $[M+H]^+$ calcd for $C_{22}H_{33}ClNO_3$ 394.2143, found 394.2141. IR ($cm^{-1}$) $\nu$ 3419, 3228, 2925, 2851, 1644, 1569, 1448, 1263, 1174. Crystal system monoclinic, space group P $2_1$/n, $a$ = 11.1541(2) Å, $b$ = 12.9126(3) Å, $c$ = 17.2790(3) Å, β = 97.560(1)°, V = 2467.03(8) Å$^3$, Z = 4, calculated density = 1.233 g/cm$^3$, μ = 0.30 mm$^{-1}$, $R_{int}$ = 0.036, R[$F^2 > 2\sigma(F^2)$] = 0.047, w$R(F^2)$ = 0.133, S = 1.02.

### 5.1.45. 1-(4-Amino-3-bromo-5-fluoro-2-methoxyphenyl)-3-[1-(cyclohexylmethyl)-4-piperidyl]propan-1-one (4n)

To a stirred solution of 1-(4-amino-5-fluoro-2-methoxyphenyl)-3-[1-(cyclohexylmethyl)-4-piperidyl]propan-1-one [**4e**] (70 mg, 0.184 mmol) in acetic acid (5 mL) was added NBS (33 mg, 0.184 mmol, 1.0 equiv) and the resulting mixture was stirred at room temperature for 2 h. The solvant was eliminated under reduced pressure. The resulting residue was dissolved in EtOAc and the organic solution was washed twice with saturated $NaHCO_3$ solution. The organic phase was dried over $MgSO_4$ and concentrated. The crude product was then purified on neutral alumina gel (DCM/EtOAc; gradient of elution 100/0 to 90/10) to afford 34 mg of the dihalogeno compound **(4n)**. (yield 41 %). $^1$H NMR ($CDCl_3$-*d*): 7.41 (d, $J$ = 11.5 Hz, 1H), 4.59 (br s, 2H), 3.82 (s, 3H), 2.97 (m, 2H), 2.84 (m, 2H), 2.08 (d, $J$ = 7.0 Hz, 2H), 1.82–1.60 (m, 11H), 1.46 (m, 1H), 1.29–1.13 (m, 6H), 0.85 (m, 2H). $^{13}$C NMR ($CDCl_3$-*d*) $\delta$ 198.3, 153.3 (d, $J$ = 2.4 Hz), 145.8 (d, $J$ = 239.1 Hz), 137.6 (d, $J$ = 15.6 Hz), 120.5 (d, $J$ = 4.8 Hz), 113.9 (d, $J$ = 20.4 Hz), 103.6 (d, $J$ = 4.2 Hz), 65.2, 61.3 (d, $J$ = 1.3 Hz), 53.4, 38.5, 34.6, 34.2, 31.2, 31.1, 30.1, 25.8, 25.2. $^{19}$F NMR ($CDCl_3$-*d*) $\delta$ −135.3. MS (ESI) *m/z* $[M+H]^+$ 455.19/457.17. HRMS (ESI) *m/z* $[M+H]^+$ calcd for $C_{22}H_{33}BrFN_2O_2$ 455.1709, found 455.1714. IR ($cm^{-1}$) $\nu$ 3472, 3362, 2921, 2850, 1670, 1619, 1493, 1450, 1405.

### 5.1.46. 1-(4-Amino-5-fluoro-3-iodo-2-methoxyphenyl)-3-[1-(cyclohexylmethyl)-4-piperidyl] propan-1-one (4o)

Similarly prepared from 1-(4-amino-5-fluoro-2-methoxyphenyl)-3-[1-(cyclohexylmethyl)-4-piperidyl]propan-1-one [**4e**] (77 mg, 0.196

mmol), acetic acid (5 mL) and NIS (30 mg, 0.196 mmol, 1.0 equiv). Yellow oil. (74 % yield). $^{1}$H NMR ($CDCl_3$-*d*): 7.41 (d, $J = 11.5$ Hz, 1H), 4.66 (br s, 2H), 3.77 (s, 3H), 2.96 (m, 2H), 2.86 (m, 2H), 2.09 (d, $J = 7.0$ Hz, 2H), 1.82 (m, 2H), 1.74 (m, 2H), 1.71–1.59 (m, 7H), 1.47 (m, 1H), 1.31–1.10 (m, 6H), 0.86 (m, 2H). $^{13}$C NMR ($CDCl_3$-*d*) $\delta$ 199.5 ($J = 1.0$ Hz), 156.7 ($J = 2.0$ Hz), 145.8 ($J = 200.0$ Hz), 141.1 ($J = 12.3$ Hz), 121.3 ($J = 3.9$ Hz), 116.1 ($J = 17.3$ Hz), 82.3 ($J = 2.3$ Hz), 66.1, 62.7 ($J = 1.1$ Hz), 54.4, 39.2, 39.2, 35.6, 35.2, 32.1, 31.2, 26.8, 26.2. $^{19}$F NMR ($CDCl_3$-*d*) $\delta$ −134.5. MS (ESI) *m/z* $[M+H]^+$ 502.75. HRMS (ESI) *m/z* $[M+H]^+$ calcd for $C_{22}H_{33}FIN_2O_2$ 503.1571, found 503.1580. IR ($cm^{-1}$) $\nu$ 3466, 3359, 2921, 2850, 1667, 1617, 1484, 1398.

### 5.1.47. 1-(4-Amino-5-fluoro-2-methoxyphenyl)-3-[1-(cyclohexylmethyl)-4-piperidyl]propan -1-one, fumarate salt

A mixture of 1-(4-amino-5-fluoro-2-methoxyphenyl)-3-[1-(cyclohexylmethyl)-4-piperidyl]propan-1-one [**4a**] (151 mg, 0.402 mmol), fumaric acid (47 mg, 0.402 mmol, 1 equiv) and isopropanol (5 mL) was refluxed during 1 h. After cooled at room temperature, the precipitate was isolated by filtration and washed with $Et_2O$. Pale yellow powder (61 % yield). mp 167−169 °C. $^{1}$H NMR (DMSO-$d_6$) $\delta$ 7.32 (d, $J = 12.7$ Hz, 1H), 6.55 (s, 2H), 6.41 (d, $J = 7.3$ Hz, 1H), 6.10 (br s, 2H), 3.79 (s, 3H), 3.01 (m, 2H), 2.82 (m, 2H), 2.34 (d, $J = 7.0$ Hz, 2H), 2.18 (m, 2H), 1.74–1.54 (m, 8H), 1.47 (m, 2H), 1.28–1.09 (m, 6H), 0.85 (m, 2H). $^{13}$C NMR (DMSO-$d_6$) $\delta$ 197.3, 167.4, 157.8, 145.1 (d, $J = 230.2$ Hz), 143.1 (d, $J = 14.8$ Hz), 135.0, 116.1 (d, $J = 19.3$ Hz), 114.0 (d, $J = 3.7$ Hz), 98.4 (d, $J = 4.2$ Hz), 63.6, 56.2, 53.3, 40.5, 34.3, 33.7, 31.3, 31.0, 31.4, 30.4, 26.4, 25.7. MS (ESI) *m/z* $[M + H]^+ = 377.62$. IR ($cm^{-1}$) $\nu$ 3437, 3342, 3225, 2926, 2856, 1653, 1637, 1592, 1526, 1439, 1315.

### 5.1.48. 1-(4-Amino-2-ethoxy-5-iodophenyl)-3-[1-(cyclohexylmethyl)-4-piperidyl]propan-1-one [4p]

To a stirred solution of 1-(4-amino-2-ethoxyphenyl)-3-[1-(cyclohexylmethyl)-4-piperidyl]propan-1-one [**4d**] (44 mg, 0.118 mmol) in peracetic acid (acetic acid/30 % $H_2O_2$ 2/1, 50 mL/mmol) was added NaI (20 mg, 0.130 mmol, 1.1 equiv) and the resulting mixture was stirred at room temperature for 2h. The reaction was cooled at 0 °C in an ice-water bath, and were added respectively water and saturated $Na_2S_2O_3$ solution. The mixture was then neutralized by addition of 2 N NaOH solution until basic pH (~10), and extracted several times with DCM. The combined organic extract was dried over $MgSO_4$ and was concentrated *in vacuo*. The residue was purified by chromatography on silica gel column and concentrated under reduced pressure to afford iodinated compound as a yellow solid (11 mg, 18 % yield). mp 97–99 °C. $^{1}$H NMR ($CDCl_3$-*d*) $\delta$ 8.11 (s, 1H), 6.23 (s, 1H), 4.53 (br s, 2H, $NH_2$), 4.05 (q, $J = 6.9$ Hz, 2H), 3.29 (m, 2H), 2.95 (t, $J = 7.2$ Hz, 2H), 2.57 (m, 2H), 2.40 (m, 2H), 1.88–1.64 (m, 10H), 1.51 (m, 1H), 1.46 (t, $J = 7.0$ Hz, 3H), 1.30–1.09 (m, 5H), 1.01 (m, 2H). $^{13}$C NMR ($CDCl_3$-*d*) $\delta$ 198.3, 160.7, 151.7, 142.0, 120.3, 97.2, 73.3, 64.7, 64.3, 54.0, 40.4, 33.9, 32.0, 29.8, 29.8, 29.8, 26.1, 25.9, 14.9. MS (ESI) *m/z* $[M+H]^+$ 499.52. HRMS (ESI) *m/z* $[M+H]^+$ calcd for $C_{23}H_{36}IN_2O_2$ 499.1816, found 499.1817. IR ($cm^{-1}$) $\nu$ 3429, 3187, 2924, 2851, 1625, 1575, 1436, 1260, 1211, 1189, 1039.

### 5.1.49. 1-[4-Amino-2-(2-fluoroethoxy)-5-iodophenyl]-3-[1-(cyclohexylmethyl)-4-piperidyl] propan-1-one (4q)

Similarly prepared from 1-[4-amino-2-(2-fluoroethoxy)phenyl]-3-[1-(cyclohexyl methyl)-4-piperidyl]propan-1- one [**4e**] (77 mg, 0.197 mmol), stirring the reaction for 1h at room temperature. After a purification by flash chromatography on silica gel column (cyclohexane/EtOAc, gradient of elution 100/0 to 20/80), the compound **(4q)** was obtained as a pale yellow solid (42 mg, 41 % yield). mp 128–130 °C. $^{1}$H NMR ($CDCl_3$-*d*) $\delta$ 8.13 (s, 1H), 6.21 (s, 1H), 4.78 (dt, $J = 47.4$ Hz, $J = 4.0$ Hz, 2H), 4.49 (br s, 2H, $NH_2$), 4.22 (dt, $J = 4.1$ Hz, $J = 27.5$ Hz, 2H), 2.95 (t, $J = 7.6$ Hz, 2H), 2.83 (m, 2H), 2.07 (d, $J = 7.0$ Hz, 2H), 1.83–1.56 (m, 11H), 1.47 (m, 1H), 1.25–1.09 (m, 6H), 0.85 (m, 2H). $^{13}$C NMR ($CDCl_3$-*d*) $\delta$ 199.0, 159.8, 151.3, 142.2, 120.9, 97.4, 81.5 (d, $J = 171.6$ Hz), 74.1, 67.8 (d, $J = 20.2$ Hz), 66.4, 54.7, 41.2, 36.0, 35.4, 32.4, 32.3, 31.3, 27.0, 26.4. $^{19}$F NMR ($CDCl_3$-*d*) $\delta$ −223.3 (tt, $J = 47.4$ Hz, $J = 27.4$ Hz). MS (ESI) *m/z* $[M+H]^+$ 517.53. HRMS (ESI) *m/z* $[M+H]^+$ calcd for $C_{23}H_{35}FIN_2O_2$ 517.1722, found 517.1722. IR ($cm^{-1}$) $\nu$ 3459, 3320, 3203, 2920, 2845, 1637, 1569, 1430, 1214, 1071, 899.

### 5.1.50. N-[2-chloro-5-methoxy-4-[1-oxo-3-(1-(cyclohexylmethyl)-4-piperidyl)propyl] phenyl]acetamide (4r)

A solution of 77 mg of donecopride (0.196 mmol) in 3 mL of acetic anhydride was stirred at room temperature overnignt. The solution was then concentrated. The resulting residue was dissolved in EtOAc and washed twice with sat $NaHCO_3$. The organic phase was dried over $MgSO_4$ and concentrated under reduced pressure. The crude product was then purified on neutral alumina gel (DCM/AcOEt, gradient of elution 100/0 to 90/10) to afford 65 mg of the product as a white solid (76 % yield). mp 82–84 °C. $^{1}$H NMR ($CDCl_3$-*d*) $\delta$ 8.28 (s, 1H), 7.79 (s, 1H), 7.77 (br s, 1H, NH), 3.92 (s, 3H), 2.94 (m, 2H), 2.84 (m, 2H), 2.27 (s, 3H), 2.07 (d, $J = 7.0$ Hz, 2H), 1.82–1.57 (m, 11H), 1.46 (m, 1H), 1.27–1.08 (m, 6H), 0.86 (m, 2H). $^{13}$C NMR ($CDCl_3$-*d*) $\delta$ 200.1, 168.6, 158.4, 138.6, 130.7, 123.6, 113.6, 103.9, 66.3, 56.0, 54.5, 41.2, 35.7, 35.3, 32.3, 32.2, 31.1, 26.8, 26.2, 25.2. MS (ESI) *m/z* $[M + H]^+ =$ 435.29/437.27. HRMS (ESI) *m/z* $[M+H]^+$ calcd for $C_{24}H_{36}ClN_2O_3$ 435.2414, found 435.2415. IR ($cm^{-1}$) $\nu$ 3345, 2920, 2849, 1704, 1672, 1599, 1578, 1512, 1450, 1401.

### 5.1.51. N-[2-chloro-5-hydroxy-4-[1-oxo-3-(1-(cyclohexylmethyl)-4-piperidyl)propyl] phenyl]acetamide (4s)

To a solution of compound **4r** (95 mg, 0.150 mmol) in DCM was added at 0 °C a solution of $BBr_3$ (1 M in DCM, 660 µL 4 equiv) and the mixture was then stirred overnight at room temperature. A saturated $NaHCO_3$ solution was added and the 2 phases are separated. The organic phase was washed with water, dried over $MgSO_4$, filtrated and concentrated under reduced pressure. The crude product was then purified on silica gel (gradient of elution: DCM to DCM/MeOH/$NH_3$ aq 95/5/1 %) to afford 30 mg of the product **(4s)** as a white solid (48 % yield). mp 167–169 °C. $^{1}$H NMR ($CDCl_3$-*d*) $\delta$ 12.42 (br s, 1H), 8.15 (s, 1H), 7.76 (br s, 1H, NH), 7.71 (s, 1H), 2.94–2.90 (m, 4H), 2.84 (m, 2H), 2.26 (s, 3H), 2.16 (m, 2H), 1.92 (m, 2H), 1.76 (m, 2H), 1.72–1.64 (m, 7H), 1.52 (m, 1H), 1.36 (m, 1H), 1.26–1.12 (m, 3H), 0.88 (m, 2H). $^{13}$C NMR ($CDCl_3$-*d*) $\delta$ 203.3, 167.3, 161.8, 139.6, 128.7, 114.4, 110.8, 108.4, 64.9, 53.3, 34.3, 34.2, 34.0, 31.0, 30.7, 29.7, 25.7, 25.1, 24.1. MS (ESI) *m/z* $[M+H]^+$ 421.56/423.55. HRMS (ESI) *m/z* $[M+H]^+$ calcd for $C_{23}H_{34}ClN_2O_3$ 421.2258, found 421.2263. IR ($cm^{-1}$) $\nu$ 3401, 2922, 2852, 1744, 1687, 1637, 1578, 1515, 1405.

### 5.1.52. 1-(4-Amino-5-chloro-2-hydroxyphenyl)-3-[1-(cyclohexylmethyl)-4-piperidyl] propan -1-one (4t)

Similarly prepared from donecopride (147 mg, 0.375 mmol), a solution of $BBr_3$ (1 M in DCM, 1.125 mL, 3 equiv) and DCM (3 mL) with 1 h stirring at room temperature. White solid (82 % yield). mp 123–125 °C. $^{1}$H NMR ($CD_3OD$-$d_4$) $\delta$ 7.74 (s, 1H), 6.23 (s, 1H), 3.13 (m, 2H), 2.92 (m, 2H), 2.43 (m, 2H), 2.27 (m, 2H), 1.86–1.64 (m, 9H), 1.47 (m, 1H), 1.41–1.29 (m, 6H), 1.27–1.22 (m, 2H), 0.98 (m, 2H). $^{13}$C NMR ($CD_3OD$-$d_4$) $\delta$ 203.1, 163.4, 151.9, 130.9, 110.5, 109.1, 99.8, 65.0, 53.7, 34.5, 34.2, 34.1, 31.4, 30.8, 30.4, 26.1, 25.6. MS (ESI) *m/z* $[M + H]^+ =$ 379.59/381.58. HRMS (ESI) *m/z* $[M+H]^+$ calcd for $C_{21}H_{32}ClN_2O_2$ 379.2152, found 379.2134. IR ($cm^{-1}$) $\nu$ 3471, 3368, 2921, 2849, 1637, 1506, 1379.

### 5.1.53. 1-(4-Amino-5-chloro-2-ethoxyphenyl)-3-[1-(cyclohexylmethyl)-4-piperidyl]propan-1-one (4u)

To a stirred solution of 1-(4-amino-5-chloro-2-hydroxyphenyl)-3-[1-(cyclohexylmethyl)-4-piperidyl]propan-1-one **(4t)** (66 mg, 0.159 mmol) in DMF (5 mL) were added $K_2CO_3$ (44 mg, 0.317 mmol, 2.0 equiv) and iodoethane (15 µL, 0.190 mmol, 1.2 equiv), then the resulting mixture was stirred at 70 °C overnight. After cooling to room temperature, the mixture was concentrated *in vacuo*. The crude was dissolved with EtOAc,

then the organic layer was washed with brine, dried over $MgSO_4$ and concentrated *in vacuo*. The crude was purified by chromatography on neutral alumina gel column (DCM/EtOAc, gradient 100:0 to 90:10) to afford the product **(4u)** as beige solid (47 % yield). mp 146–148 °C. $^1$H NMR ($CDCl_3$-*d*) $\delta$ 7.77 (s, 1H), 6.22 (s, 1H), 4.43 (br s, 2H), 4.03 (qd, $J$ = 7.0 Hz, 2H), 2.93 (m, 2H), 2.83 (m, 2H), 2.07 (d, $J$ = 7.0 Hz, 2H), 1.81 (m, 2H), 1.74 (m, 2H), 1.70–1.63 (m, 5H), 1.58 (m, 2H), 1.50–1.44 (m, 4H), 1.28–1.10 (m, 6H), 0.85 (m, 2H). $^{13}$C NMR ($CDCl_3$-*d*) $\delta$ 199.4, 158.9, 147.6, 132.1, 119.2, 111.2, 98.2, 66.3, 64.3, 54.6, 41.2, 35.9, 35.3, 32.3, 32.1, 31.3, 26.8, 26.2, 14.8. MS (ESI) *m/z* $[M + H]^+$ = 407.65/409.64. HRMS (ESI) *m/z* $[M+H]^+$ calcd for $C_{23}H_{36}ClN_2O_2$ 407.2465, found 407.2468. IR ($cm^{-1}$) $\nu$ 3436, 2926, 2854, 1621, 1436, 1260, 1201.

#### 5.1.54. 1-[4-Amino-5-chloro-2-(2-fluoroethoxy)phenyl]-3-[1-(cyclohexylmethyl)-4-piperidyl]propan-1-one (4v)

Similarly prepared from 1-(4-amino-5-chloro-2-hydroxyphenyl)-3-[1-(cyclohexylmethyl)-4-piperidyl]propan-1-one **(4t)** (72 mg, 0.190 mmol), 2-fluoroethyl-4-methylbenzene-1-sulfonate (50 mg, 0.229 mmol, 1.2 equiv), $K_2CO_3$ (53 mg, 0.381 mmol, 2 equiv) and DMF (5 mL). Brown solid (31 % yield). mp 138–140 °C. $^1$H NMR ($CDCl_3$-*d*) $\delta$ 7.79 (s, 1H), 6.24 (s, 1H), 4.77 (m, 2H), 4.50 (br s, 2H), 4.22 (m, 2H), 2.96 (m, 2H), 2.89 (m, 2H), 2.13 (m, 2H), 1.89 (m, 2H), 1.75 (m, 2H), 1.70–1.62 (m, 4H), 1.60 (m, 2H), 1.50 (m, 1H), 1.42 (m, 1H), 1.35–1.10 (m, 6H), 0.86 (m, 2H).$^{13}$C NMR ($CDCl_3$-*d*) $\delta$ 199.0, 158.1, 147.6, 132.3, 119.3, 111.9, 98.4, 81.4 ($J$ = 142.7 Hz), 67.8 ($J$ = 16.8 Hz), 66.0, 54.4, 41.1, 35.6, 35.1, 32.1, 31.9, 31.0, 26.7, 26.2. MS (ESI) *m/z* $[M + H]^+$ = 425.28/427.27. HRMS (ESI) *m/z* $[M+H]^+$ calcd for $C_{23}H_{35}ClFN_2O_2$ 425.2371, found 425.2377. IR ($cm^{-1}$) $\nu$ 3432, 2927, 2676, 1679, 1619, 1587, 1434.

#### 5.1.55. 1-[4-Amino-5-chloro-2-(methoxy-$d_3$)phenyl]-3-[1-(cyclohexylmethyl)-4-piperidyl] propan-1-one (4w)

Similarly prepared from 1-(4-amino-5-chloro-2-hydroxyphenyl)-3-[1-(cyclohexylmethyl)-4-piperidyl]propan-1-one **(4t)** (55 mg, 0.144 mmol), iodomethane-$d_3$ (10 µL, 0.158 mmol, 1.1 equiv), $K_2CO_3$ (24 mg, 0.173 mmol, 1.2 equiv) and DMF (3 mL) with an overnight stirring at room temperature. Yellow solid (21 % yield). mp 152–154 °C. $^1$H NMR ($CDCl_3$-*d*) $\delta$ 7.78 (s, 1H), 6.25 (s, 1H), 4.45 (br s, 2H, $NH_2$), 2.91–2.87 (m, 2H), 2.85–2.83 (m, 2H), 2.07 (d, $J$ = 7.1 Hz, 2H), 1.84–1.55 (m, 11H), 1.49 (m, 1H), 1.31–1.11 (m, 6H), 0.85 (m, 2H). $^{13}$C NMR ($CDCl_3$-*d*) $\delta$ 199.3, 159.5, 147.6, 132.2, 119.0, 111.2, 97.5, 66.3, 54.6, 41.0, 35.8, 35.3, 32.3, 32.2, 31.4, 31.0, 26.8, 26.2. MS (ESI) *m/z* $[M + H]^+$ = 396.26/398.26. HRMS (ESI) *m/z* $[M+H]^+$ calcd for $C_{22}H_{31}D_3ClN_2O_2$ 396.2497, found 396.2497. IR ($cm^{-1}$) $\nu$ 3483, 3328, 2919, 2848, 1640, 1623, 1574, 1437, 1214.

### 5.2. In vitro biological studies

#### 5.2.1. Pharmacological characterization of drugs on human 5-HT$_4$R

The competition studies used membrane preparations made from proprietary stable recombinant cell lines expressing the 5-HT$_4$(b) receptor to ensure high-level of GPCR surface expression (HTS110 M, Sigma Aldrich). The membranes (2.5 µg protein) were incubated in duplicate at 25 °C for 60 min in the absence or the presence of $10^{-6}$ or $10^{-8}$ M of each drug and 0.2 nM [$^3$H]-GR113808 (NET1152, Revvity) in 25 mM Tris buffer (pH 7.4, 25 °C). At the end of the incubation, the homogenates were filtered through Whatman GF/C filters (Alpha Biotech, Glasgow, Scotland) pre-soaked with 0.5 % polyethyleneimine using a Brandel cell harvester. The filters were subsequently washed three times with ice-cold 50 mM Tris buffer (pH7.4, 4 °C). Non-specific binding was evaluated in parallel in the presence of 30 µM serotonin. For some of these compounds, the affinity constants were calculated from five-point inhibition curves using the GraphPad Prism 6 software and expressed as $K_i \pm$ SD.

#### 5.2.2. Determination of cAMP production

COS-7 cells were grown in Dulbecco's modified Eagle medium (DMEM) supplemented with 10 % dialyzed fetal calf serum (dFCS) and antibiotics. Cells were transiently transfected with plasmid encoding HA-tagged h5-HT$_4$R, then seeded in 96-well plates (16,000 cells/well). 24 hrs after transfection, cells were exposed to the indicated concentrations of 5-HT$_4$R ligands in the presence of 0.1 mM of the phosphodiesterase inhibitor RO-20-1724, at 37 °C in 250 µl of HBS (20 mM HEPES; 150 mM NaCl; 4.2 mM KCl; 0.9 mM $CaCl_2$; 0.5 mM $MgCl_2$; 0.1 % glucose; 0.1 % BSA). After 10 min, cells were then lysed by addition of the same volume of Triton-X100 (0.1 %). Quantification of cAMP production was performed by HTRF® by using the cAMP - HTRF Gs Dynamic kit (PerkinElmer, Codolet, France) according to the manufacturer's instructions.

#### 5.2.3. Determination of sAPPα production in transfected cells

COS-7 cells were transfected with plasmids encoding FLG-tagged (*h*) 5-HT$_4$ receptor and secreted placental alkaline phosphatase (SEAP, Clontech, Saint-Germain-en-Laye, France)-tagged mouse APP695 (generous gift of Dr Bernadette Allinquant), as previously described [12], and then seeded in 24-well plates (300,000 cells/well). 24 hrs after transfection, cells were incubated with the appropriate drug concentration for 30 min, then culture supernatants were collected, and SEAP activity measured by adding the chromogenic substrate *p*-nitrophenyl phosphate disodium hexahydrate (Sigma-Aldrich, Saint-Quentin Fallavier, France) according to the manufacturer's instructions. The reaction readout was performed at 405 nm (colorimetric assay) using an Infinite 200 multimode microplate reader (Tecan, Männedorf, Switzerland). This technique measures all secreted soluble forms of APP and does not discriminate between sAPPα and sAPPβ.

#### 5.2.4. In vitro tests of AChE and BuChE biological activity

Inhibitory capacity of compounds on AChE biological activity was evaluated through the use of the spectrometric method of Ellman [19]. Acetyl- or butyrylthiocholine iodide and 5,5-dithiobis-(2-nitrobenzoic) acid (DTNB) were purchased from Sigma Aldrich. Lyophilized BuChE from equine serum (Sigma Aldrich) was dissolved in 0.1 M phosphate buffer pH 7.4 such as to have enzyme solutions stock with 20 units/mL enzyme activity. AChE from human erythrocytes (buffered aqueous solution, ≥500 units/mg protein (BCA), Sigma Aldrich) or AChE recombinant (Sigma Aldrich) was diluted in 20 mM HEPES buffer pH 8, 0.1 % Triton X-100 such as to have enzyme solution with 0.25 unit/mL or 0.125 unit/mL enzyme activity respectively. In the procedure, 100 µL of 0.3 mM DTNB dissolved in phosphate buffer pH 7.4 were added into the 96 wells plate followed by 50 µL of test compound solution and 50 µL of erythrocyte enzyme (0.05 U final) or recombinant enzyme (0.025 U final) respectively. After 5 min of preincubation at 25 °C, the reaction was then initiated by the injection of 50 µL of 1 mM acetyl- or butyrylthiocholine iodide solution. The hydrolysis of acetyl- or butyrylthiocholine was monitored by the formation of yellow 5-thio-2-nitrobenzoate anion as the result of the reaction of DTNB with thiocholine, released by the enzymatic hydrolysis of acetyl- or butyrylthiocholine, at a wavelength of 412 nm using a 96-well microplate plate reader (SYNERGY 2Biotek, Colmar, France). Test compounds were dissolved in analytical grade DMSO. Donepezil or Tacrine was used as a reference standard. The rate of absorbance increase at 412 nm was followed every minute for 10 min. Assays were performed with a blank containing all components except acetyl- or butyrylthiocholine, in order to account for non-enzymatic reaction. The reaction slopes were compared and the percent inhibition due to the presence of test compounds was calculated by the following expression: 100 - (vi/v0x100) where vi is the rate calculated in the presence of inhibitor and v0 is the enzyme activity.

First screening of AChE and BuChE activity was carried out at a $10^{-6}$ or $10^{-5}$ M concentration of compounds under study. For the compounds with significant inhibition, $IC_{50}$ values were determined graphically by

plotting the % inhibition versus the logarithm of six inhibitor concentrations in the assay solution using the GraphPad Prism 6 software.

### 5.2.5. Drugability parameters

*5.2.5.1. Parallel Artificial Membrane Permeability Assay (PAMPA).* The Pampa-BBB experiments were conducted using the Pampa Explorer Kit (Pion Inc, Woburn, MA, USA) according to the protocol provided by the manufacturer. Briefly, the flucopride solution (20 mM in DMSO) was diluted in Prisma HT buffer pH 7.4 (pION) to 100 μM. 200 μL of this solution (n = 6) were added to the donor plate (P/N 110243). 5 μL of the BBB-1 Lipid (P/N 110672) was used to coat the membrane filter of the acceptor plate (P/N 110243). 200 μL of the Brain Sink Buffer (P/N 110674) was added to each well of the acceptor plate. The PAMPA sandwich was assembled and allowed to incubate at room temperature for 4 h, without stirring. The sandwich was then separated and the UV–visible spectra were measured for both the donor and receiver wells with the microplate reader (Tecan infinit M200). The -logPe and Pe were calculated by the PAMPA Explorer software v. 3.7 (pION) for studied compounds. Corticosterone (-log Pe = 4.76, Pe = $17.2.10^{-6}$ cm/s) and theophylline (-log Pe = 6.44, Pe = $0.40.10^{-6}$ cm/s) were used as positive and negative references, respectively.

The Pampa-GIT experiments were conducted using the Pampa Explorer Kit (Pion Inc) according to manufacturer's protocol. Briefly, each stock compound solution (20 mM in DMSO) were diluted in Prisma HT buffer pH 7.4, 6 or 5 (pION) to 100 μM. 200 μl of these solutions (n = 4) was added to donor plate (P/N 110243). 5 μl of the GIT-0 Lipid (P/N 110669) was used to coat the membrane filter of the acceptor plate (P/N 110243). 200 μl of the Acceptor Sink Buffer (P/N 110139) was added to each well of the acceptor plate. The sandwich was incubated at room temperature for 4 h, without stirring. After the incubation, the UV–visible spectra were measured with the microplate reader (Tecan infinit M200) and the –logPe and Pe were calculated by The PAMPA Explorer software v. 3.7 (pION) for flucopride. The antipyrine and the ketoprofen were used as reference.

*5.2.5.2. Water solubility.* Thermodynamic solubility of flucopride was determined according to the classical shake-flask method (OECD guideline n°105) and a miniaturized procedure recently described. The pH of buffer solutions was chosen according to the calculated pKa of flucopride amino group to determine the intrinsic solubility Sint (solubility of the neutral form) at pH = 12, and the solubility Sphysio in physiological conditions at pH = 7.4. Furthermore, the solubility in water Sw was determined. Buffer solutions (pH 7.4 or pH 12, 10 μM) were prepared from $K_3PO_4$, $K_2HPO_4$, $KH_2PO_4$, and by adding KCl 50 μM (Sigma Aldrich, Saint Quentin Fallavier, France). 1 mg of flucopride was added to capped glass tubes containing 4 mL of either water or buffer (n = 3). Tubes were briefly sonicated and horizontally shacked at room temperature. An immediate precipitation was observed in all tubes. After 48 h, 1 mL was sampled in a 1.5 mL microtube and centrifugated at 13,500 rpm for 5 min 100 μL of the supernatant was mixed with 100 μL of acetonitrile/DMSO (99:1, v/v) in a Greiner UV microplate. Determination of flucopride solubility was made with a Tecan Infinite M200 microplate reader in spectrophotometric mode ($\lambda_{max}$ = 326 nm) from a calibration curve obtained from four standard solutions of flucopride solubilized at 0, 12.5, 25, 50 μM in a 50:50 (v/v) mixture of water or buffer with acetonitrinile/DMSO (99:1, v/v). Calibration curves were linear with $R^2 > 0.999$. Standard solutions were prepared extemporaneously from stock solutions of flucopride solubilized in DMSO at 0, 2.5, 5 and 10 mM. 5 μL of each stock solution was diluted with 995 μL of water or buffer, and then mixed with 1 mL of acetonitrile in order to keep unchanged the final proportions of each solvent in standard solutions and in samples.

*5.2.5.3. Inhibition of P-gp efflux pump.* NCI/ADR-RES cells were maintained in complete RPMI medium, supplemented with 10 % fetal calf serum, in the presence of penicillin, streptomycin and fungizone in 75 $cm^2$ flask under 5%$CO_2$. 60,000 Cells were seeded in 200 μL medium in black 96-well tissue culture plate, before being washed with PBS 24h later and incubated for 1h at 37 °C under 5 % $CO_2$ with 100 μL medium without FCS containing 12.5 μM rhodamine 123 and tested compounds dissolved in methanol. Cells were washed three times with PBS, lysated with 20 mM Tris pH7.7, 0.2 % SDS and fluorescence monitored (ex 507 nm/em 528 nm). Cyclosporin A (10 μM) was used as positive control.

*5.2.5.4. Mutagenicity.* Preliminary screening was performed using the semi-quantitative technique (the spot test) as previously described [20] with the tester typhimurium strains (TA97a, TA98, TA100, TA102) ± 9 Mix.

*5.2.5.5. Cell culture and cell proliferation assay.* The human cell line MRC5-SV2 was grown in D-MEM medium supplemented with 10 % fetal calf serum, in the presence of penicillin, streptomycin and fungizone in 75 $cm^2$ flask under 5%$CO_2$. Cells were plated in 96-well tissue culture plates in 200 μL medium and treated 24h later with 2 μL stock solution of compounds dissolved in DMSO using a Biomek 3000 (Beckman-Coulter). Controls received the same volume of DMSO (1 % final volume). After 72 h exposure, the MTS reagent (Celltiter 96Aqueous One solution, Promega) was added and incubated for 3 h at 37 °C: the absorbance was monitored at 490 nm and results expressed as the inhibition of cell proliferation calculated as the ratio [(1-(OD490 treated/OD490 control)) × 100] in triplicate experiments.

*5.2.5.6. Metabolic stability and metabolite identification for flucopride fumarate in mouse, rat, dog and human liver microsomes. In vitro* metabolism of flucopride fumarate was investigated using incubations with human, dog, mouse and rat liver microsomes for 60 min. The collected samples were analyzed using a UPLC/QE-orbitrap-MS method developed for the purpose to monitor disappearance of the parent compound and to identify metabolites and to form metabolite profiles.

*5.2.5.7. Inhibition of CYP model activities by flucopride fumarate in human liver microsomes in vitro.* The inhibition potential of flucopride fumarate towards major drug-metabolizing CYP enzymes was studied in human liver microsomes. The inhibition potential towards CYP1A2, CYP2A6, CYP2B6, CYP2C8, CYP2C9, CYP2C19, CYP2D6 and CYP3A4 was assessed using CYP specific probe reactions in cocktail incubation. Five concentrations of flucopride fumarate (0.01, 0.1, 1, 10 and 100 μM) were used. In addition, control inhibitors for each probe reaction were incubated at single concentration above $IC_{50}$.

### 5.3. In vivo biological studies

#### 5.3.1. Animals

Adult male NMRI mice (3 months old, weighing 35–40g) from Janvier labs (Le Genest-Saint-Isle, France) were used to perform experiments. Mice were housed by ten in standard polycarbonate cages in standard controlled conditions (22 ± 2 °C, 55 ± 10 % humidity) with a reversed 12h light/dark cycle (light on at 7pm). Food and water were available *ad libitum* in the home cage. All experiments were conducted (between 9am and 3pm) during the active - dark - phase of the cycle and were in agreement with the European Directives and French law on animal experimentation (personal authorization n° 14–17 for MB and 14–60 for TF).

#### 5.3.2. Pharmacokinetic study

*5.3.2.1. Design study.* Pharmacokinetic study was performed in mouse and rat (respectively, C57Bl6 and Wistar strain). Flucopride was administered intravenously (0.3, 1, 3 mg/kg, iv.), orally (1, 3, 9 mg/kg,

per os) and intraperitoneally (0.3, 1, 3 mg/kg, ip.). Each dose was tested in three animals. The doses were prepared in 0.9 % saline and delivered in a volume of 10 and 2 mL/kg respectively for mouse and rat. Terminal blood (cardiac puncture) and CSF (cisterna magna) samplings were performed while animals were kept under isoflurane anesthesia (2–3% in a mixture of $O_2/N_2O$ 30/70). Samples were stored at −20 °C before analysis. It was then possible to evaluate pharmacokinetic parameters, oral bioavailability and CSF entry using a non-compartmental analysis (NCA).

*5.3.2.2. Standard, plasma and CSF samples treatment.* 10 or 1 μL of each working standard was spiked to a 100 μL aliquot of blank plasma or 10 μL of CSF, vortexed and incubated 30 min. Proteins precipitation was performed adding MR33583 solution as external standard (ES) at 3300 ng/mL in −20 °C ACN: 100 and 10 μL for plasma and CSF sample respectively. Samples were vortexed and incubated 20 min at 4 °C then centrifuged (10 min, 19000 g). The supernatant was filtered using 0.2 μm PTFE filters, and filtrates were directly analyzed. Final concentrations were 1, 5, 10, 25, 50, 100, 250, 500 ng/mL for flucopride fumarate standards, 25, 500 and 330 for ng/mL $IS_L$, $IS_H$ and ES.

*5.3.2.3. Chromatographic and mass spectrometry conditions.* Chromatography separation was conducted on a Nexera $X^2$ system coupled with a tandem mass spectrometer LCMS-8030 (Shimadzu, Kyoto, Japon) under the following conditions: column, Acquity HSS T3 (100 × 1 mm; 1.8 μm) (Waters, Millford, MA, USA); mobile phase, 0.05 % (v/v) formic acid in water (A) and acetonitrile (B) with gradient elution (0–1.20min, 15 % B; 1.20–1.21 min, 15–70 % B; 1.21–3.20 min, 70 % B; 3.20–3.21 70-15 % B); flow rate, 0.3 mL/min; column temperature, 55 °C; injection volume, 0.6 μL. The MS/MS detection was performed by electrospray ionization (ESI) source operated in positive mode. The multiple reactions monitoring (MRM) was used for the detection and quantification of precursors to product ion transition. Two MRM transitions (qualifier and quantifier) were used for each analyte and standard. The capillary voltage and source temperature were maintained at 4,5 kV and 350 °C, respectively whereas desolvation temperature was 250 °C. Highly pure nitrogen was used as desolvation gas (10 L/min) whereas argon gas was used for collision gas pressure (230 KPa). The optimized MRM parameters for analytes and IS are listed in Table 1. The data acquisition was ascertained by LabSolution (Version 5.86 SP1) software.

*5.3.2.4. Calibration.* Calibration curves were established by plotting the ratios of peak high of each analyte to $IS_L$ or $IS_H$ *versus* the plasma concentrations based on weighted quadratic least-squares regression model (1/x). The lower limits of quantification (LLOQ) under present UHPLC–MS/MS conditions were 1 ng/mL for flucopride determined on the basis of response at a signal-to-noise ratio of 10:1.

*5.3.2.5. PK calculations.* Flucopride concentration was plotted with GraphPad® Prism (version 6.01, GraphPad® Software, La Jolla, CA, USA). Main pharmacokinetic parameters were calculated: area under the plasma drug concentration-time curve ($AUC_{0-\infty}$) using the linear trapezoidal method, time to reach the maximum plasma drug concentration ($T_{max}$), maximum plasma drug concentration ($C_{max}$) and mean transit time (MTT), by non-compartmental analysis using "R" version 3.4.0 software [21] equipped with "PK" package version 1.3–3 [22]. Relative bioavailability F of oral administration versus i.p. was calculated according to the following equation: $F = (AUC_{po}/AUC_{ip}) \times (Dose_{ip}/Dose_{po})$.

*5.3.3. CNS-activity and acute toxicity test*

Behavioral and neurological changes induced by graded doses (1, 10, 100 mg/kg) of the tested derivatives were evaluated in groups of four mice, by a standardized observation technique at different times (30 min, 3 and 24 h) after ip. administration [23]. Major changes of behavioral data (for example, hypo- or hyperactivity, ataxia, tremors, convulsion, etc.) were noted in comparison to the control group. The dose that induced first adverse effect was noticed. Amphetamine (2 mg/kg), chlorpromazine (10 mg/kg) were used as stimulant and depressive references, respectively.

*5.3.3.1. Locomotor activity.* Locomotor activity was measured using an actimeter (Imetronic®) through infrared detection. Mice were placed in individual removable polycarbonate cages (21 cm length, 7 cm wide and 12 cm high). Locomotor activity was measured by recording the number of interruption of beams of the red light over a period of 30min through an attached recording system to the actimeter. Flucopride fumarate was tested at 1, 3 and 10 mg/kg. Amphetamine (2 mg/kg), chlorpromazine (10 mg/kg) and association Donepezil (DPZ) (0.3 mg/kg) - RS 67333 (RS) (0.1 mg/kg) were used as stimulant, depressive and pharmacological references, respectively [24].

*5.3.3.2. Spatial working memory.* Anti-amnesiant activity of tested compounds was evaluated by reversal of scopolamine (0.5 mg/kg) - induced deficit on spontaneous alternation behavior in the Y maze test [25]. The Y maze made of grey plastic consisted of three equally spaced arms (21-cm long, 7-cm wide with walls 15-cm high). The mouse was placed at the end of one of the arms and allowed to move freely through the maze during a 5 min session while the sequence of arm entries was recorded by an observer. An arm entry was scored when all four feet crossed into the arm. An alternation was defined as entries into all three arms on a consecutive occasion. The number of possible alternation is thus the total number of arm entries minus two; the percentage of alternation was calculated as (actual alternation/possible alternation) 100. Flucopride fumarate was tested at 0.3, 1 and 10 mg/kg. Association DPZ (0.3 mg/kg)-RS (0.1 mg/kg) was tested as pharmacological reference.

*5.3.3.3. Object recognition memory.* The test procedure [26,27] consisted in three sessions: familiarization, acquisition, and retention. During the first 3 days, mice were familiarized to the arena for 5 min per day. The test began on day 4. Acquisition consisted in a 3-min session in which two identical objects were placed in the box. After a 72-h inter-trial interval, the mouse was placed again in the same arena (retention session), in which one of the two objects, was replaced by a novel object. The exploration time of each object for each animal was collected manually by an experimenter blind to the treatment group, and the discrimination index [(time spent exploring novel object − time exploring familiar object)/(time spent exploring novel object + time exploring familiar object)] was calculated. Object exploration was considered when the nose of the animal was directed towards the object at a distance below 2 cm. Mice that did not explore any of the two objects at the acquisition session were excluded from the data analysis. Flucopride fumarate was tested at 0.3, 1 and 10 mg/kg. Association DPZ (0.3 mg/kg)-RS (0.1 mg/kg) was tested as pharmacological reference.

*5.3.3.4. Pharmacological treatments.* RS 67333 and Donepezil hydrochloride were purchased from Tocris® (Cookson, UK). Amphetamine [(+)-α-Methylphenethylamine] hemisulfate, chlorpromazine hydrochloride, and scopolamine hydrobromide were purchased from Sigma (France). All those pharmacological compounds were dissolved in NaCl 0.9 % as the vehicle were administered intraperitoneally 30 min before tests, except scopolamine which was subcutaneously administered 20 min before tests.

*5.3.3.5. Statistical analysis.* Results were expressed as mean ± SD and were analyzed by one-way analysis of variance (ANOVA), with Statview® software. In case of significance, a SNK (Student-Newman-Keuls) *post hoc* test was realized. Additionally, for the spontaneous alternation test, the percentage of alternation was compared to a theoretical 50 %

value (random alternation) by a univariate *t-test*. For the object recognition test, exploration times (familiar versus new objects) were compared by a univariate *t-test* and discrimination index were compared to a theoretical 0 value (no discrimination performance) by an univariate *t-test*. Differences were considered as statistically significant if the *p* value was strictly under 0.05.

## CRediT authorship contribution statement

**Christophe Rochais:** Conceptualization. **Cédric Lecoutey:** Investigation. **Julien Lalut:** Data curation. **Audrey Davis:** Data curation. **Emilie Duval:** Funding acquisition. **Florence Gaven:** Data curation. **Stacy Largillière:** Data curation. **Gérald Née:** Data curation. **Sophie Corvaisier:** Data curation. **Jana Sopkova de Oliveira Santos:** Data curation. **Marc Since:** Data curation. **Thomas Freret:** Data curation. **Romain Legrand:** Funding acquisition. **Noëlle Callizot:** Data curation. **Sylvie Claeysen:** Conceptualization. **Michel Boulouard:** Conceptualization. **Patrick Dallemagne:** Conceptualization.

## Conflict of interest

N Callizot is co-founder of Neuro-Sys, member of the scientific board and consulting for: Alzprotect, Inflectis, Axoltis, Raya Therapeutics, Neuralia, Cerenys.

R Legrand, C Rochais and P Dallemagne are co-founders and members of the scientific board of RonomA-Pharma.

## Declaration of competing interest

The authors declare the following financial interests/personal relationships which may be considered as potential competing interests:

Patrick Dallemagne has patent #Acetylcholinesterase inhibitor compounds and 5-HT4 serotonergic receptor agonists with promnesia effect, their preparation and pharmaceutical compositions containing them pending to licensee. If there are other authors, they declare that they have no known competing financial interests or personal relationships that could have appeared to influence the work reported in this paper.

## Acknowledgment

This work was supported by funding from Normandie Valorisation (Preclinicalz program) and the Fondation Vaincre Alzheimer (Trevidic donation), France. The authors gratefully acknowledge the Normandie Region, France, as well as the European Community (FEDER) for the equipment of the CERMN's platform DRUID.

## Appendix A. Supplementary data

Supplementary data to this article can be found online at https://doi.org/10.1016/j.ejmech.2024.116975.

## ABBREVIATIONS

AD, Alzheimer's disease; ACh, acetylcholine; AChE, acetylcholinesterase; ARIA, amyloid related imaging abnormalities; BuChE, butyrylcholinesterase; FDA, Food and Drug Administration; MTDL, multitarget directed ligands; PAS, peripheral anionic site; BBB, blood-brain barrier; PAMPA, parallel artificial membrane permeability Assay; P-gp, P-glycoprotein; CSF, cerebrospinal fluid; AUC, area under the curve; ip., intraperitoneal; iv., intravenous; po., per os; DPZ, donepezil; CPZ, chlorpromazine; AMP, amphetamine; NORT, novel object recognition test; SAR, structure-activity relationship.

## Data availability

Data will be made available on request.

## References

[1] M. Gupta, D.F. Weaver, Alzheimer's: the ABCDE Paradigm, ACS Chem. Neurosci. 13 (9) (2022) 1355–1357, https://doi.org/10.1021/acschemneuro.2c00195.
[2] C. Song, J. Shi, P. Zhang, Y. Zhang, J. Xu, L. Zhao, R. Zhang, H. Wang, H. Chen, Immunotherapy for Alzheimer's disease: targeting β-amyloid and beyond, Transl. Neurodegener. 11 (1) (2022) 1–17, https://doi.org/10.1186/s40035-022-00292-3.
[3] S. Budd Haeberlein, P.S. Aisen, F. Barkhof, S. Chalkias, T. Chen, S. Cohen, G. Dent, O. Hansson, K. Harrison, C. von Hehn, T. Iwatsubo, C. Mallinckrodt, C. J. Mummery, K.K. Muralidharan, I. Nestorov, L. Nisenbaum, R. Rajagovindan, L. Skordos, Y. Tian, C.H. van Dyck, B. Vellas, S. Wu, Y. Zhu, A. Sandrock, Two randomized phase 3 studies of aducanumab in early alzheimer's disease, J. Prev. Alzheimers Dis. 9 (2) (2022) 197–210, https://doi.org/10.14283/jpad.2022.30. PMID:35542991.
[4] R. Perneczky, F. Jessen, T. Grimmer, J. Levin, A. Flöel, O. Peters, L. Froelich, Anti-amyloid antibody therapies in Alzheimer's disease, Brain 146 (3) (2023) 842–849, https://doi.org/10.1093/brain/awad005.
[5] C.H. van Dyck, C.J. Swanson, P. Aisen, R.J. Bateman, C. Chen, M. Gee, M. Kanekiyo, D. Li, L. Reyderman, S. Cohen, L. Froelich, S. Katayama, M. Sabbagh, B. Vellas, D. Watson, S. Dhadda, M. Irizarry, L.D. Kramer, T. Iwatsubo, Lecanemab in early alzheimer's disease, N. Engl. J. Med. 388 (1) (2023) 9–21, https://doi.org/10.1056/NEJMoa2212948.
[6] J.R. Sims, J.A. Zimmer, C.D. Evans, M. Lu, P. Ardayfio, J.D. Sparks, A.M. Wessels, S. Shcherbinin, H. Wang, E.S. Monkul Nery, E.C. Collins, P. Solomon, S. Salloway, L.G. Apostolova, O. Hansson, C. Ritchie, D.A. Brooks, M. Mintun, D.M. Skovronsky, Donanemab in early symptomatic alzheimer disease: the TRAILBLAZER-ALZ 2 randomized clinical trial, JAMA 330 (6) (2023) 512–527, https://doi.org/10.1001/jama.2023.13239.
[7] M.A. Mintun, A.C. Lo, C. Duggan Evans, A.M. Wessels, P.A. Ardayfio, S. W. Andersen, S. Shcherbinin, J. Sparks, J.R. Sims, M. Brys, L.G. Apostolova, S. P. Salloway, D.M. Skovronsky, Donanemab in early alzheimer's disease, N. Engl. J. Med. 384 (18) (2021) 1691–1704, https://doi.org/10.1056/NEJMoa2100708.
[8] S. Sato, N. Hatakeyama, S. Fujikoshi, S. Katayama, H. Katagiri, J.R. Sims, Donanemab in Japanese patients with early alzheimer's disease: subpopulation analysis of the TRAILBLAZER-ALZ 2 randomized trial, Neurol. Ther (2024), https://doi.org/10.1007/s40120-024-00604-x.
[9] C. Lecoutey, D. Hedou, T. Freret, P. Giannoni, F. Gaven, M. Since, V. Bouet, C. Ballandonne, S. Corvaisier, A. Malzert Freon, S. Mignani, T. Cresteil, M. Boulouard, S. Claeysen, C. Rochais, P. Dallemagne, Design of donecopride, a dual serotonin subtype 4 receptor agonist/acetylcholinesterase inhibitor with potential interest for Alzheimer's disease treatment, Proc. Natl. Acad. Sci. 111 (36) (2014) E3825–E3830, https://doi.org/10.1073/pnas.1410315111.
[10] C. Rochais, C. Lecoutey, F. Gaven, P. Giannoni, K. Hamidouche, D. Hedou, E. Dubost, D. Genest, S. Yahiaoui, T. Freret, V. Bouet, F. Dauphin, J. Sopkova de Oliveira Santos, C. Ballandonne, S. Corvaisier, A. Malzert-Fréon, R. Legay, M. Boulouard, S. Claeysen, P. Dallemagne, Novel multitarget-directed ligands (MTDLs) with acetylcholinesterase (AChE) inhibitory and serotonergic subtype 4 receptor (5-ht4r) agonist activities as potential agents against Alzheimer's disease: the design of donecopride, J. Med. Chem. 58 (7) (2015) 3172–3187, https://doi.org/10.1021/acs.jmedchem.5b00115.
[11] C. Rochais, C. Lecoutey, K. Hamidouche, P. Giannoni, F. Gaven, E. Cem, S. Mignani, K. Baranger, T. Freret, J. Bockaert, S. Rivera, M. Boulouard, P. Dallemagne, S. Claeysen, Donecopride, a Swiss army knife with potential against Alzheimer's disease, Br. J. Pharmacol. 177 (9) (2020) 1988–2005, https://doi.org/10.1111/bph.14964.
[12] M. Cochet, R. Donneger, E. Cassier, F. Gaven, S.F. Lichtenthaler, P. Marin, J. Bockaert, A. Dumuis, S. Claeysen, 5-$HT_4$ receptors constitutively promote the non-amyloidogenic pathway of APP cleavage and interact with ADAM10, ACS Chem. Neurosci. 4 (1) (2013) 130–140, https://doi.org/10.1021/cn300095t.
[13] P. Giannoni, F. Gaven, D. de Bundel, K. Baranger, E. Marchetti-Gauthier, F. S. Roman, E. Valjent, P. Marin, J. Bockaert, S. Rivera, S. Claeysen, Early administration of RS 67333, a specific 5-$HT_4$ receptor agonist, prevents amyloidogenesis and behavioral deficits in the 5XFAD mouse model of Alzheimer's disease, Front. Aging Neurosci. 5 (2013) 96, https://doi.org/10.3389/fnagi.2013.00096.
[14] Y. Nagaya, Y. Nozaki, O. Takenaka, R. Watari, K. Kusano, T. Yoshimura, H. Kusuhara, Investigation of utility of cerebrospinal fluid drug concentration as a surrogate for interstitial fluid concentration using microdialysis coupled with cisternal cerebrospinal fluid sampling in wild-type and Mdr1a(−/−) rats, Drug Metab. Pharmacokinet. 31 (1) (2016) 57–66, https://doi.org/10.1016/j.dmpk.2015.10.003.
[15] R. Kuwano, H. Kusano, Benzyl protection of phenols under neutral conditions: palladium-catalyzed benzylations of phenols, Org. Lett. 15 (2008) 1979–1982, https://doi.org/10.1021/ol800548t.
[16] P. Liu, L. Huang, M.M. Faul, A simple method for chemoselective phenol alkylation, Tetrahedron Lett. 48 (41) (2007) 7380–7382, https://doi.org/10.1016/j.tetlet.2007.08.0.
[17] S. Danishefsky, C.-F. Yan, R.K. Singh, R.B. Gammill, Jr.P.M. McCurry, N. Fritsch, J. Clardy, Derivatives of 1-methoxy-3-trimethylsilyloxy-1,3-butadiene for diels-alder reactions, J. Am. Chem. Soc. 101 (1979) 7001–7008.

[18] J. Lalut, B.B. Tournier, T. Cailly, C. Lecoutey, S. Corvaisier, A. Davis, C. Ballandonne, M. Since, P. Millet, F. Fabis, P. Dallemagne, C. Rochais, Synthesis and evaluation of novel serotonin 4 receptor radiotracers for single photon emission computed tomography, Eur. J. Med. Chem. 116 (2016) 90–101, https://doi.org/10.1016/j.ejmech.2016.03.059.
[19] G.L. Ellman, K.D. Courtney, V. Andres jr, R.M. Featherstone, A new and rapid colorimetric determination of acetyl-cholinesterase activity, Biochem. Pharmacol. 7 (1961) 91–95.
[20] D.M. Maron, B.N. Ames, Revised methods for the Salmonella mutagenicity test, Mutat. Res. 113 (1983) 173–215, https://doi.org/10.1016/0165-1161(83)90010-9.
[21] R Core Team. R, The R Project for Statistical Computing, R Foundation for Statistical Computing, Vienna, Austria, 2016. https://www.r-project.org/, 2023-11-13.
[22] T. Jaki, M.J. Wolfsegger, Package "PK": basic non-compartmental pharmacokinetics. http://cran.nexr.com/web/packages/PK/, 2016, 2023-11-13.
[23] C. Morpugo, A new design for the screening of CNS-active drugs in mice, Arzneim. Forsch. 11 (1971) 1727–1734.
[24] T. Freret, V. Bouet, A. Quiedeville, G. Nee, P. Dallemagne, C. Rochais, M. Boulouard, Synergistic effect of acetylcholinesterase inhibition (donepezil) and 5-HT(4) receptor activation (RS67333) on object recognition in mice, Behav. Brain Res. 230 (2012) 304–308, https://doi.org/10.1016/j.bbr.2012.02.012.
[25] N. Hooper, C. Fraser, T. Stone, Effect of purines analogues on spontaneous alternation in mice, Psychopharmacology 123 (1996) 250–257, https://doi.org/10.1007/BF02246579.
[26] M. Leger, A. Quiedeville, V. Bouet, B. Haelewyn, M. Boulouard, P. Schumann-Bard, T. Freret, Object recognition test in mice, Nat. Protoc. 8 (2013) 2531–2537, https://doi.org/10.1038/nprot.2013.155.
[27] T. Freret, V. Bouet, A. Quiedeville, G. Nee, P. Dallemagne, C. Rochais, M. Boulouard, Synergistic effect of acetylcholinesterase inhibition (donepezil) and 5-HT(4) receptor activation (RS67333) on object recognition in mice, Behav. Brain Res. 230 (2012) 304–308, https://doi.org/10.1016/j.bbr.2012.02.012.